RESEARCH ARTICLE

Amyloid-β specific regulatory T cells attenuate Alzheimer's disease pathobiology in APP/PS1 mice

Pravin Yeapuri[1†], Jatin Machhi[1†], Yaman Lu[1], Mai Mohamed Abdelmoaty[1], Rana Kadry[1], Milankumar Patel[1], Shaurav Bhattarai[1], Eugene Lu[1], Krista L. Namminga[1], Katherine E. Olson[1], Emma G. Foster[1], R. Lee Mosley[1] and Howard E. Gendelman[1*]

Abstract

Background Regulatory T cells (Tregs) maintain immune tolerance. While Treg-mediated neuroprotective activities are now well-accepted, the lack of defined antigen specificity limits their therapeutic potential. This is notable for neurodegenerative diseases where cell access to injured brain regions is required for disease-specific therapeutic targeting and improved outcomes. To address this need, amyloid-beta (Aβ) antigen specificity was conferred to Treg responses by engineering the T cell receptor (TCR) specific for Aβ ($TCR_{Aβ}$). The TCR_{Ab} were developed from disease-specific T cell effector (Teff) clones. The ability of Tregs expressing a transgenic $TCR_{Aβ}$ ($TCR_{Aβ}$ -Tregs) to reduce Aβ burden, transform effector to regulatory cells, and reverse disease-associated neurotoxicity proved beneficial in an animal model of Alzheimer's disease.

Methods $TCR_{Aβ}$ -Tregs were generated by CRISPR-Cas9 knockout of endogenous TCR and consequent incorporation of the transgenic TCR_{Ab} identified from Aβ reactive Teff monoclones. Antigen specificity was confirmed by MHC-Aβ-tetramer staining. Adoptive transfer of $TCR_{Aβ}$-Tregs to mice expressing a chimeric mouse-human amyloid precursor protein and a mutant human presenilin-1 followed measured behavior, immune, and immunohistochemical outcomes.

Results $TCR_{Aβ}$-Tregs expressed an Aβ-specific TCR. Adoptive transfer of $TCR_{Aβ}$-Tregs led to sustained immune suppression, reduced microglial reaction, and amyloid loads. ^{18}F-fluorodeoxyglucose radiolabeled $TCR_{Aβ}$-Treg homed to the brain facilitating antigen specificity. Reduction in amyloid load was associated with improved cognitive functions.

Conclusions $TCR_{Aβ}$-Tregs reduced amyloid burden, restored brain homeostasis, and improved learning and memory, supporting the increased therapeutic benefit of antigen specific Treg immunotherapy for AD.

Keywords Treg cell therapy, Alzheimer's disease, Immunotherapy, Antigen specific, T cell receptor, Amyloid beta

---

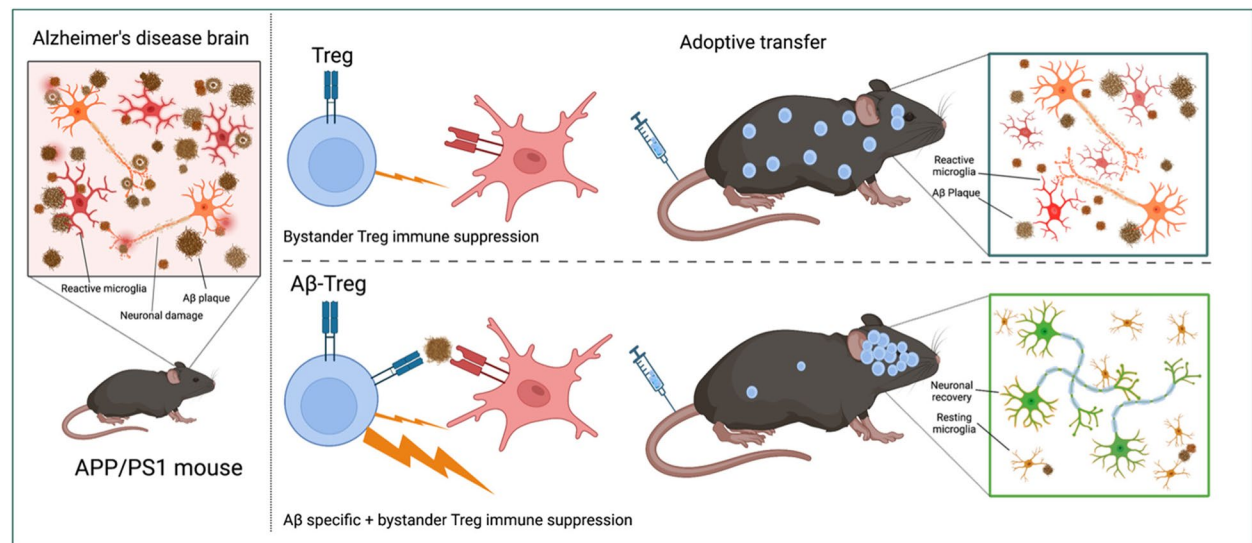[†]Pravin Yeapuri and Jatin Machhi contributed equally to this work.

*Correspondence:
Howard E. Gendelman
hegendel@unmc.edu
Full list of author information is available at the end of the article

Yeapuri *et al. Molecular Neurodegeneration*   (2023) 18:97

Page 2 of 22

Graphical Abstract

Background

Alzheimer's disease (AD) is the most common neurodegenerative disorder [1]. Disease is clinically manifest by progressive cognitive decline. Pathologically, disease progression is linked to deposition of extracellular amyloid β (Aβ) plaque deposition, intracellular neurofibrillary tangles, and neuroinflammation [2]. Current drug regimens provide only symptomatic benefit and are ineffective at halting progression of disease [3, 4]. Disease-modifying treatments have used active or passive immunization to clear Aβ plaques. While each proved successful at reducing plaque burden and cognitive defects in animals, [5–7] human trials showed limited success with adverse reactions following immunizations. Study cessation was mandated after active immunization due to the development of meningoencephalitis in a few of the treated patients [8]. This was attributed to the emergence of effector T cells (Teffs) [8–10]. CD4+ Teffs induced by Aβ vaccination produced disease-associated Aβ-specific type-1 T helper (Th1) cells [11].

Thus, the effectiveness of active immunization remains, at present, uncertain. This includes the deployment of Th2-biased adjuvants or by limiting the length of the Aβ epitope to avoid neurotoxic T cell responses [12, 13] [14]. Regrettably, such strategies do not generate stable T cell phenotypes and may elicit undesired Teff responses. The development of optimal neuroprotective immune responses, especially in aged patients, who possess weakened or compromised immune systems remains challenging [15]. Currently, two passive Aβ-specific monoclonal antibody therapies, aducanumab and lecanemab, have US Food and Drug Administration (FDA) approval for AD treatments but have shown more limited success and high prevalence of adverse events due to amyloid-related imaging abnormalities (ARIA) edemas and effusions [16–19].

Given each of these limitations for immunization-based disease-modifying AD therapeutics, T cell and chimeric antigen receptor-based therapies (TCR and CAR-T) are attractive therapeutic alternatives. Notably, T cell-based therapies, using assorted T effector phenotypes, have produced remarkable clinical outcomes in the field of cancer [20, 21]. However, given the adverse events observed with Th1 induction during active immunization strategies, T cell-based therapy for AD required a new directive. This was found through the deployment of regulatory T cells (Tregs). While Tregs are well known to maintain immunological tolerance during disease, such tolerance may be altered. In disease states, Teffs react to misfolded Aβ deposits, clonally expand, then affect neuroinflammation and AD neuropathology [22–25]. Such responses were observed in AD patients before onset of disease symptoms [22, 24, 26, 27]. Our own works have shown that adoptive transfer of Aβ-reactive Teffs accelerate amyloid pathology and cognitive defects in mice expressing chimeric mouse/human amyloid precursor and a mutant human presenilin 1 protein (APP/PS1) [28, 29].

The path forward focused on harnessing CD4+ Tregs for neuroprotection [28]. This novel idea provides a

Yeapuri *et al. Molecular Neurodegeneration*   (2023) 18:97

Page 3 of 22

specific immune signature in ameliorating disease due to Treg's vibrant anti-inflammatory and immunosuppressive activities [28–35]. Treg-inducing agents or, adoptive transfer of polyclonal Tregs confer protection in diverse neurodegenerative diseases. These include but are not limited to AD, stroke, Parkinson's disease (PD), and amyotrophic lateral sclerosis [28, 35–40]. However, such polyclonal Tregs could also lead to global immune suppression and consequent increased prevalence of infectious or neoplastic diseases. Thus, Tregs specific for disease-inducing pathological proteins such as Aβ, could overcome nonspecific immune dysregulation and be ideal to drive disease-specific Treg therapy which could be expanded further in a wide range of neurodegenerative diseases.

With these goals in mind, we investigated whether Tregs expressing a TCR specific for Aβ ($TCR_{Aβ}$-Tregs) attenuate AD in APP/PS1 mice. We hypothesized that $TCR_{Aβ}$-Tregs target amyloid-rich regions in brain that lead to neuroprotective outcomes. Tregs were specifically engineered for Aβ reactivity using an Aβ-specific TCR identified from Aβ-specific monoclonal Teffs [41]. In an APP/PS1 AD model, we now show that $TCR_{Aβ}$-Tregs target the brain. This results in increased reduction of reactive microglia numbers and composition concomitant with increased amyloid plaque clearance and improved cognitive outcomes.

Methods

Knockout of endogenous TCR

Polyclonal Tregs were isolated from non-transgenic mice using the EasySep™ mouse Treg enrichment kit (cat. 18,783, Stemcell Technologies, Cambridge, MA), per the manufacturer's instructions. Tregs were maintained in culture using 1:1 ratio of mouse T cell activating CD3/CD28 Dynabeads (cat. 11456D, Thermo Fisher Scientific, Waltham, MA) and 1000 IU/mL IL-2 (cat. 212–12, Peprotech, Cranbury, NJ) in complete RPMI-1640 media supplemented with 10% fetal bovine serum (FBS), 2 mM L-glutamine, 25 mM HEPES, 1 mM sodium pyruvate, 1×nonessential amino acids, 55 nM 2-mercaptoethanol, 100 U/mL penicillin, and 100 µg streptomycin (complete RPMI-1640). The endogenous TCRs of isolated polyclonal Tregs were deleted using CRISPR-Cas9 technology. Guide RNAs (gRNAs) targeting the TCR alpha (U*A*U*GGAUUCCAAGAGCAAUG) and TCR beta (U*G*G*GGUCAGCACGGACCCUC) region and Cas9 nuclease were obtained from Sythego, Redwood city, California. To delete endogenous TCRs, 50 µM (pmoles/µL) of each guide RNA in 1XTris-EDTA (10mMTris, 1mMEDTA, 0.2µ filtered) was mixed with 20 µM (pmoles/µL) Cas9 and electroporated into cultured Tregs using 4D-nucleofector™ X unit (cat.

AAF-1003X, Lonza, Basel, Switzerland) according to the manufacturer's mouse T cell protocol. Briefly, TCR-alpha, and TCR-beta gRNAs (1µL, 100 pmol stock) and Cas9 (2µL, 40 pmol stock) were incubated in a 0.5 mL microcentrifuge tube for 5 min. Simultaneously, $2×10^6$ Tregs were collected in a 0.5 mL microcentrifuge tube and resuspended in 16 µL of P3 nucleofector solution (cat. V4XP-3032, Lonza, Basel, Switzerland). The gRNAs preincubated with Cas9 mixture was mixed with Tregs in a total volume of ~20 µL. This mixture was transferred to one well in the Primary Cell 4D-Nucleofector™ X Kit S (cat. V4XP-3032. Lonza, Basel, Switzerland) and electroporated using the DN-100 program. Immediately after electroporation, 100 µL warm complete RPMI-1640 media was added to the well and incubated at 37 °C for 15 min to help cells recover. Cells were then collected and plated in 24 well plates with 1:1 Dynabeads and 1000 IU/mL IL-2 in complete RPMI-1640 media. Cells were analyzed for TCR knockout using anti-TCRα/β-PE antibody (cat. LS-C76264, LSBio, Shirley, MA) by flow cytometry. TCR knockout Tregs (TCR⁻⁻-Tregs) were sorted for anti-TCRα/β-PE negative cells and maintained in 1:1 ratio Dyna beads and 1000 IU/mL IL-2. Sustained deletion of endogenous TCRs was confirmed by flowcytometry for ~2–3 weeks.

Generation of $TCR_{Aβ}$-Treg

To generate $TCR_{Aβ}$-Tregs, a plasmid construct encoding the $TCR_{Aβ}$ previously identified by our laboratory from Aβ-reactive Teff monoclones [41] was electroporated into TCR⁻⁻-Tregs at either 0.5 µL or 0.25 µL of 1.56 µg/µL of the plasmid construct. For the in vitro evaluation of $TCR_{Aβ}$-Tregs, $2×10^6$ TCR⁻⁻-Treg were collected into a 0.5 mL microcentrifuge tubes, resuspended in ~20 µL P3 nucleofector solution (cat. V4XP-3032, Lonza, Basel, Switzerland) and mixed with either 0.5 µL or 0.25 µL of 1.56 µg/µL of a $TCR_{Aβ}$ plasmid. The mixture was transferred into the Primary Cell 4D-Nucleofector™ X Kit S (cat. V4XP-3032. Lonza, Basel, Switzerland) and electroporated using the DN-100 program as previously described. For the animal studies, TCR⁻⁻-Tregs electroporated with 0.5 µL of 1.56 µg/µL of $TCR_{Aβ}$ plasmid construct was used. Incorporation of the $TCR_{Aβ}$ to TCR⁻⁻-Tregs after electroporation was confirmed using anti-TCRα/β-PE antibody (cat. LS-C76264, LSBio, WA). To confirm Aβ specificity of the engineered Tregs, tetramers of $Aβ_{1-42}$ T cell epitopes presented by H-2^b haplotypes were constructed with I-A^b and the Aβ amino acid 15–30 (MHCII-IA^b–KLVFFAEDVGSNKGA) conjugated to fluorophore BV421 (National Institute of Health (NIH) Tetramer Core Facility, Emory University, Atlanta, GA). MHCII-IA^b–PVSKMRMATPLLMQA tetramer with irrelevant peptide was used as control.

For tetramer staining, 3×10^5 TCR$_{A\beta}$-Tregs or polyclonal Tregs were incubated with MHCII-IA^b–KLVFFAEDVG-SNKGA Aβ tetramer (2.4 μg) or MHCII-IA^b–PVSKMR-MATPLLMQA control tetramer (2.4 μg) for 3 h at 37 °C. After incubation, tetramer-stained T cells were reacted with anti-CD3e-PE and anti-CD4-APC-H7 antibodies for 30 min at room temperature, followed by live-dead staining with propidium iodide (0.5 μg/ml) for 5 min at room temperature. Stained T cells were analyzed with a LSR II flow cytometer and FACSDiva Software (BD Bioscience) at the University of Nebraska Medical Center (UNMC) Flow Cytometry Research Facility. To evaluate the cytokine profile of the engineered cells, 1×10^6 TCR$_{A\beta}$-Tregs, polyclonal Tregs, or TCR^{--}-Tregs were stimulated with PMA (20 ng/mL) and ionomycin (1 μM) overnight in complete RPMI-1640 media. Cell supernatants were collected, and cytokine profile evaluated using mouse cytokine array kit (cat. ARY006, R&D systems, Minneapolis, MN) following manufacturer's instructions. The films were developed and imaged on iBright CL1500 imaging systems (Invitrogen, Waltham, MA) and average signal (pixel density) was analyzed using ImageJ software. For controls, TCR^{--}-Tregs were electroporated with plasmid vector without TCR construct (empty vector, EV) generating EV-Tregs.

TCR$_{A\beta}$ lentiviral constructs

The lentiviral constructs for transducing the TCR$_{A\beta}$ into target cells were performed as previously described [42]. Lentivirus construct containing the TCR$_{A\beta}$ along with lentiviral packaging mix were co-transfected into HEK293FT cells using Lipofectamine™ 3000 Transfection Reagent (cat. L3000001, Thermofisher, Waltham, MA) according to manufacturer's instructions. Following incubation, the cell supernatants containing the TCR$_{A\beta}$ lentiviral constructs were purified by passing through 0.45 μm filters and concentrated by ultracentrifugation at $100,000 \times g$ for 1 h. The viral stock titered against HEK293FT cells yielded a titer of 10^9 transduction units/mL. Transdux-Max (cat. LV860A-1, System Biosciences, Palo Alto, CA) was used for the transduction of the TCR$_{A\beta}$ lentiviral constructs into TCR^{--}-Treg, human PBMC's, HEK293FT and CEM-SS cells according to manufacturer's instructions. Successful transduction and expression of TCR$_{A\beta}$ was confirmed by tetramer staining with MHCII-IA^b–KLVFFAEDVGSNKGA as previously described.

Adoptive Cell Transfer in APP/PS1 mice

All animal experiments were approved by the Institutional Animal Care and Use Committee of the UNMC. Transgenic mice overexpressing human APP695 with the Swedish mutation (Tg2576) were obtained from Drs. G. Carlson and K. Hsiao-Ashe through the Mayo Medical Venture [43]. PS1 mice overexpressing human PS1 with M146L mutation were provided by Dr. K. Duff from the University of South Florida [44]. Both mice were maintained on the B6;129 hybrid background. Male Tg2576 mice were crossbred with female PS1 mice to generate APP/PS1 double-transgenic mice and non-transgenic (non-Tg), and B6;129 mice were developed in parallel, as described previously [35, 45–47]. Female APP/PS1 mice, 8 months old, and age-matched non-transgenic littermates were blindly randomized into different experimental groups. Either 1×10^6 TCR$_{A\beta}$-Tregs, polyclonal Tregs, or EV-Tregs (TCR^{--}-Tregs electroporated with empty plasmid vector) in 100 μL phosphate-buffered saline (PBS) were adoptively transferred to APP/PS1 recipient mice, intravenously via tail vein using a 28-gauge needle affixed to a sterile tuberculin syringe, thrice at 1-week intervals. Both the engineered Tregs (TCR$_{A\beta}$-Tregs and EV-Tregs) and polyclonal Tregs were maintained and amplified using 1:1 ratio of anti-CD3/CD28 Dynabeads and 1000 IU/mL IL-2 prior to adoptive transfer. Both age-matched untreated APP/PS1 mice and non-transgenic mice served as controls.

Radial arm water and Y-maze tests

After the third adoptive cell transfer, mice were submitted for radial arm water maze (RAWM) testing in a blinded fashion to assess memory impairment as previously described [35, 48]. Briefly, mice from masked cages were introduced into the circular water filled tank (diameter-110 cm and height-91 cm, San Diego Instruments) with triangular inserts that produce six swim paths radiating from the center. Special cues are fixed on the tank wall to guide mouse orientation. At the end of any one arm, a circular plexiglass hidden platform (diameter-10 cm) is submerged 1 cm beneath the water level. The platform was placed in the same arm for four consecutive acquisition trials (T1–T4), and retention trial (T5), but in a different arm on different experimental days. For T1–T4, the mouse started the task from a randomly chosen arm without a platform. After four trials, the mouse was returned to its cage for 30 min and reintroduced into the T4 arm, for the delayed retention trial (T5). Each trial lasted 1 min, and an error was scored when the mouse entered the wrong arm; entered the arm with the platform, but did not climb on it; or did not make a choice for 20 s. The trial ended when the mouse climbed and stayed on the platform for at least 10 s. The mouse was allowed to rest on the platform for 20 s between trials. If the mouse did not climb the platform, after 60 s, it was gently guided to the submerged platform. The T1, T4 and T5 trial errors over 9-day test were divided into three blocks (block-1 days 1–3, block-2 days 4–6, block-3 days 7–9),

Yeapuri *et al. Molecular Neurodegeneration*   (2023) 18:97

Page 5 of 22

and the errors in each block were averaged for statistical analysis. We used the Y-maze test to evaluate spatial learning and memory using the short-term alterations method [49]. The arms of the maze had 39.5*8.5*13 cm dimensions with 120° angle between the arms. Mice were allowed to explore the maze freely for 8 min, and the total entries were recorded visually. Successful entries were defined as consecutive entries into three different arms.

^{18}F-FDG cell tracking

To confirm migration and accumulation of Tregs to the brain, $TCR_{A\beta}$-Tregs or polyclonal Tregs were radiolabeled with ^{18}F-fluorodeoxyglucose (^{18}F-FDG, Cardinal Health, Omaha, NE). Briefly, cells were glucose starved by incubating them in glucose-free RPMI-1640 media (cat. 11,879–020, Gibco-Thermo Fisher Scientific, Waltham, MA) for 4 h at 37 °C. Following starvation, cells were incubated with a previously optimized non-toxic concentration, 1 mCi/mL ^{18}F-FDG, for 1 h at 37 °C to allow uptake of radioactive glucose. Neither the 4 h glucose starvation nor the 1 mCi/mL ^{18}F-FDG had a marked effect on cell viability. Cells were then washed thrice to remove excess radioactive compound and 5×10^6 cells/mouse were injected intravenously via the tail vein to 8-month-old APP/PS1 and allowed 10 min for uptake. Radioactivity was measured using combined positron emission tomography (PET/CT) (β-Cube, Molecubes Inc., Lexington, MA) at 0.5, 2, 4 and 6 h in the UNMC PET Core Facility. Briefly, mice were anesthetized with 2% isoflurane with oxygen. Acquisition time of 10 min was used at time points 0.5, 2, 4, and 6-h post-injection to measure radioactivity. Computed tomography (CT) scans were acquired using TriFoil imaging Triumph (Tri-foil imaging Northridge, CA). The X-ray tube was used at 150 μA and 75 kV. Each run obtained 512 projections with an exposure time of 230 ms. VIVOQUANT software (inviCRO, Boston, MA) was used to overlay and analyze CT and PET reconstructed images. The 3D brain atlas software was used for quantifying radioactivity from different brain regions.

Brain glucose uptake

Mice were fasted overnight and ^{18}FDG (Cardinal Health, Omaha, NE) was injected intravenously to fasted mice, and brain glucose uptake was evaluated by PET scan. Briefly, mice were anesthetized by 2% isoflurane along with oxygen. ^{18}FDG with an activity of 70 μCI in a total volume of 0.1 ml PBS was intravenously injected into the lateral tail vein and allowed for 10 min of uptake. At 30 min post-injection, 10 min PET acquisitions were carried out using Molecube beta-CUBE (MOLECUBES NV, Gent, Belgium). CT scans were acquired using Tri-Foil imaging Triumph (Tri-foil imaging Northridge, CA). The X-ray tube was used at 150 μA and 75 kV. Each run obtained 512 projections with an exposure time of 230 ms. VIVOQUANT software (inviCRO, Boston, MA) was used to overlay the CT and PET reconstructed images for glucose uptake measurements.

Measures of Treg function

Comparison of Treg function of the engineered Treg cells or systemic Tregs from different mice treatments was performed as described earlier [50]. For evaluating systemic Treg function, Tregs (CD4+CD25+) and Tresp (T responder) (CD4+CD25−) cells were isolated from the mice spleens using EasySep™ mouse Treg enrichment kit (Cat. 18,783, Stemcell Technologies, Vancouver, CA), per the manufacturer's instructions, and CD4+T cells were enriched from splenic single cell suspension by negative selection using the EasySep™ mouse CD4+T cell isolation cocktail. From the enriched CD4+populations, CD25+cells were positively selected using the EasySep™ mouse CD25+Treg selection cocktail. The isolated CD4+CD25+cells were more than 97% FOXP3+as determined by flow cytometric analysis. The CD4+CD25− Tresps, more than 96% pure, were collected from naïve non-Tg mice spleens and used in the proliferation assay. Briefly, Tresp cells were labeling with carboxyfluorescein succinimidyl ester (CFSE) (Cat. C34554, Thermo Fisher Scientific, Waltham, MA). CD4+CD25+Tregs from different treatment groups were serially diluted in a U-bottom 96-well plate to obtain 50, 25, 12.5, and 6.25×10^3 Tregs in 100 μl of media followed by addition of 50×10^3 CFSE-labeled Tresp cells from non-Tg mice into each well to obtain Treg:Tresp ratios of 1:1, 0.5:1, 0.25:1 and 0.125:1. Wells with only Tresps served as controls. Mouse T cell activating CD3/CD28 Dynabeads (Catalog no. 11456D, Thermo Fisher Scientific) were added to each well at a bead:Tresp ratio of 1:1 to induce Tresp proliferation. Tresp cells alone with and without Dynabeads served as controls for baseline Tresp proliferation without Treg suppression. The immunosuppressive function of Tregs to inhibit proliferation of CFSE-stained Tresps was determined after 72 h incubation at 37 °C using flow cytometric analysis and is reported as Treg-mediated % inhibition: [1-(Percent proliferation of Tresp:Treg dilution ÷ Percent proliferation of stimulated Tresp alone)] × 100. For comparing Treg function of the engineered Tregs, ex-vivo cultured Tregs or $TCR_{A\beta}$-Treg collected on day 2 after electroporation of TCR^{--}-Tregs with 0.25 μL or 0.5 μL of 1.56 μg/mL the $TCR_{A\beta}$ plasmid were co-incubated with CFSE-labeled Tresp cells from non-Tg mice at a ratio of 1:1, 0.5:1, 0.25:1 and 0.125:1 Treg:Tresp for 72 h days and suppressive function was evaluated by flowcytometry as described earlier.

Yeapuri *et al. Molecular Neurodegeneration*   (2023) 18:97

Page 6 of 22

Antigen (Aβ) specific treg function

To evaluate antigen mediated Treg function of the engineered TCR$_{Aβ}$-Treg cells, CFSE labelled Tresp cells isolated from non-Tg mice were stimulated overnight with CD3/CD28 Dynabeads at 1:1 bead:Tresp cell ratio in a 48 well plate. Dynabeads were magnetically removed to isolate pre-stimulated CFSE-labeled Tresp cells. In a 96 well U bottom plate, 50×10^3 pre-stimulated CFSE-labeled Tresp were co-incubated with an equal number of ex-vivo cultured Tregs, or TCR$_{Aβ}$-Tregs collected on Day-2 post electroporation with 0.5 µL of 1.56 µg/mL TCR$_{Aβ}$ plasmid. For antigen stimulation, 5µL of Aβ-MHC tetramer (1.16 mg/mL) was added per well and incubated for 72 h. Pre-stimulated CFSE labelled Tresp alone or un-stimulated CFSE-labeled Tresp were used as controls for baseline Tresp proliferation. The antigen mediated immunosuppressive function of Tregs to inhibit proliferation of pre-stimulated CFSE-stained Tresp cells was determined using flow cytometric analysis and is reported as Treg-mediated percent inhibition: [1-(percent proliferation of 1:1 Tresp:Treg dilution ÷ percent proliferation of pre-stimulated Tresp alone)] × 100.

Flow cytometry

On day of sacrifice, pentobarbital was used to terminally anesthetize the mice. Spleens were harvested into complete RPMI-1640 media and blood collected by cardiac puncture in K$_3$EDTA tubes (cat. 450,475, Greiner BioOne North America, Monroe, NC). Mice were then pericardially perfused with PBS, and brains and lymph nodes (axial, cervical and inguinal) were harvested. To isolate immune cells from brain, brain tissues were homogenized in Hanks' balanced salt solution (HBSS) and passed through a 70 µm cell strainer. Cells were centrifuged and resuspended in 500µL HBSS and incubated with 100 µL DNAase and 100 µL collagenase for 5 min at 37 °C. After incubation, cells were centrifuged, resuspended in 4 mL 30% Percoll, layered with 4 mL HBSS, centrifuged (700xg for 10 min), and the cell pellet collected for flow staining. Single cell suspensions of splenocytes (10^6 cells), lymph nodes (10^6 cells), or whole blood (50 µL) were used for flow staining. To determine the frequency of Tregs in different organs, 10^6 cells were incubated at room temperature for 30 min in 100 µL PBS/1% BSA/0.09% NaN3 with PE-anti-CD3e (cat. 12–0031-81, Invitrogen, Waltham, MA), APC-H7-anti-CD4 (cat. 560,181, BD Pharmingen), PE-Cyanine5.5-anti-CD8a (cat.35–0081-82, Invitrogen), PE-Cy7-anti-CD25 (cat. 25–0251-82, eBioscience, San Diego, CA), and Alexa Fluor 488-anti-FOXP3 (cat. 320,012, BioLegend, San Diego, CA). Isotypes and FMO (fluorescence-minus-one) were used for accurate gating. To determine the frequency of Aβ reactive CD4+T cells, 1×10^6 lymph node cells were stimulated with Aβ$_{1–42}$ (25 µg/ml) in presence of feeder cells (irradiated splenocytes) and IL-2 (20 IU/mL) for 5 days at 37 °C. On day 5, cells were collected by centrifugation and incubated Live/Dead™ Fixable Blue Dye (cat. L23105, Thermo Fisher Scientific) followed by MHCII-IA^b–KLVFFAED-VGSNKGA Aβ tetramer (6 µg) or MHCII-IA^b–PVSKM-RMATPLLMQA control tetramer (6 µg) for 3 h at 37 °C. After incubation, live/dead stained T cell-MHCII-Aβ tetramer complexes were stained with PE-anti-CD3e, APC-H7-anti-CD4, PE-Cyanine5.5-anti-CD8a, PE-, and Alexa Fluor 488 labeled anti-FOXP3 for flow cytometric analysis.

Immunohistochemistry

After transcardial perfusion, brains were immediately harvested and divided into two hemispheres. The left was immediately frozen on dry ice for biochemical analysis and the right was immersed in fresh, depolymerized 4% paraformaldehyde in PBS for 48 h at 4 °C and cryoprotected by immersion in 15% then 30% sucrose for 24 h/immersion at 4 °C. Fixed brains were sectioned coronally with a cryostat (Thermo Fisher Scientific), and 30 µm sections were serially collected and stored at −80 °C. Immunohistochemistry was performed using antibodies against pan-Aβ (1:500, rabbit polyclonal, cat. 715,800, Thermo Fisher Scientific), Iba1 (1:1000, rabbit polyclonal, cat. 01919741, Wako Chemicals, Richmond, VA) and doublecortin (Dcx) (1:500, goat polyclonal, cat. Sc8066, Santa Cruz Biotechnology, Dallas, TX). For immunodetection, biotin-conjugated anti-rabbit or anti-goat IgG secondary antibody was used followed by a tertiary incubation with Vectastain ABC Elite kit (cat. PK6100, Vector Laboratories, Newark, CA). One percent thioflavin-S in 50% ethanol was used for counterstaining of compact amyloid plaque (cat. T1892, Sigma-Aldrich, St. Louis, MO). For each of the immunohistochemical staining, six sections/slide were collected at eight intervals and were used for each of the experimental groups. Slides were masked and coded, and Aβ occupied area was calculated using Cavalieri estimator probe (grid spacing 15 µm), while the number of Iba1-reactive microglia cells were counted using the Optical Fractionator probe of Stereo Investigator system (MBF Bioscience, Williston, VT) as described earlier [45]. Briefly, a high-sensitivity digital camera (OrcaFlash2.8, Hamamatsu C11440-10C, Hamamatsu, Japan) interfaced with a Nikon Eclipse 90i microscope (Nikon, Melville, NY, USA) was used. Within the Stereo Investigator, the contour in each section was delineated using a tracing function. While sections showed tissue shrinkage along the anteroposterior axis, the extent of shrinkage between sections from different animals was similar. The dimensions for the counting frame (120 × 100 µm) and the grid size (245 × 240 µm)

Yeapuri *et al. Molecular Neurodegeneration*   (2023) 18:97

Page 7 of 22

were set. The z-plane focus was adjusted at each section for clarity. Immunoreactive cells were marked positive in each counting frame and quantified by the software based on the section parameters and marked cell counts.

Aβ detection by ELISA

Snap-frozen mouse cortex was homogenized in 50 mM Tris–HCL (pH 7.6) containing 150 mM of NaCl and a protease inhibitor. Lysates were centrifuged at $20,000 \times g$ for 60 min at 4 °C, and the supernatants were collected for detecting soluble fraction of $A\beta_{42}$. For detecting insoluble fractions of $A\beta_{42}$, pellets were dissolved using 6 M guanidine-HCL and were centrifuged at the same speed and time at room temperature. $A\beta_{1-42}$ loads in the brain cortex were quantified using an ELISA kit (Quantikine ELISA, cat. DAB142, R & D Systems, Minneapolis, MN) following the manufacturer's protocol.

RNA extraction and qPCR

RNA was extracted from the brain cortexes using RNeasy Mini Kit (Qiagen, cat 74,101, Hilden, Germany) following the manufacturer's protocol. Extracted RNA was quantified using NanoDrop One (Thermo Scientific, cat ND-ONE-W, Waltham, MA). For cDNA preparation, 1ug RNA was reverse transcribed using a TaqMan reverse transcription kit (Applied Biosystems, cat N808080234, Waltham, MA). Prepared cDNA was diluted 1:5 for downstream qPCR assay. For the qPCR assay, TaqMan Gene Expression Master Mix kit (Applied Biosystems, cat 4,369,016, Waltham, MA) was used to quantify the relative expression of ITGAX, Clec7A, GFAP, and TREM2 genes. Similarly, RPLP0 gene was used as the reference gene. Commercially available predesigned murine primers were purchased from Integrated DNA Technologies, Coralville, IA (Primer sequences provided in Supplementary data, Table 2). Relative gene expression was calculated using the delta-delta cycle threshold method $(2 - \Delta\Delta Ct)$ [51].

Statistical analysis

All data were normally distributed and presented as mean values ± standard errors of the mean (SEM). Comparisons of means between groups were analyzed by one-way ANOVA or two-way repeated measures ANOVA followed by Turkey's post hoc test using Graph-Pad Prizm software version 8.0 (GraphPad Software, San Diego, CA). A value of $p \leq 0.05$ was regarded as a significant difference.

Results

Generation of Aβ-specific Tregs

Our prior studies demonstrated the pathobiological role of Aβ-specific T effector cells (Aβ-Teffs) in APP/PS1 mice. The high-affinity Aβ-Teff clones were generated following immunization of mice with $A\beta_{1-42}$ [41]. The TCR identified from Aβ-Teff clones were used to design $TCR_{A\beta}$ plasmid constructs for lentiviral transduction of Treg recipient cells. As a first step toward engineering, the endogenous TCRs of polyclonal Treg primary isolates were deleted by CRISPR-Cas9 technology. Guide RNAs (gRNAs) encoding the α- and β- chains of the TCR were electroporated into polyclonal Tregs isolated from non-transgenic mice (Fig. 1A). This resulted in the deletion of TCRs on more than 95% of Tregs. TCR knockout Treg cells (TCR^{--}-Tregs) were flow-sorted and the stability of TCR deletions was confirmed by flow cytometric analysis every week for over a month. As a first step for transduction, the lentiviral approach was used to facilitate $TCR_{A\beta}$ entry into TCR^{--}-Tregs. The produced lentiviral construct was able to transfect human PBMC's, CEMSS and HEK-293 cells with the $TCR_{A\beta}$ (Fig S1,2). However, as lentiviruses poorly transduce mouse T cells, stable transduction of mouse Tregs with $TCR_{A\beta}$ lentiviral constructs was not successful (Fig S1). To overcome this limitation, $TCR_{A\beta}$ encoding plasmids (Fig. 1B) were electroporated into TCR^{--}-Tregs to generate $TCR_{A\beta}$-Tregs. While electroporation of the $TCR_{A\beta}$ encoding plasmid led to significant cell death within 24 h, surviving cells recovered by day-2 and flow cytometric analysis showed stable expression of the TCR for 4–6 days following electroporation (Fig. 1C, D). Aβ specificity of the $TCR_{A\beta}$ was confirmed by flow cytometry of the $TCR_{A\beta}$-Tregs and increased staining of MHCII-IA[b]–KLVFFAE-DVG-SNKGA tetramer (Fig. 1E).

To assess the functionality of $TCR_{A\beta}$-Tregs, we determined their ability to suppress proliferation of T

(See figure on next page.)
Fig. 1 *Generation of $TCR_{A\beta}$-Tregs*. **A**. Flow cytometry gating confirming the CRISPR-Cas9-mediated knockout of endogenous T cell receptors (TCRs) to generate TCR^{--}-Tregs. Nucleotide sequences represent the guide RNAs targeting the alpha and beta regions of the TCR. **B**. Plasmid design for $TCR_{A\beta}$ electroporation. **C**. Representative gating strategy confirming the TCR expression by TCR-Tregs electroporated with 0.5 μL of TCR$_{A\beta}$ plasmid (plasmid conc. = 1.5 μg/μL). **D**. Time course of $TCR_{A\beta}$ expression on engineered $TCR_{A\beta}$-Tregs post electroporation with $TCR_{A\beta}$ plasmid. Phenotype characterization of engineered $TCR_{A\beta}$-Tregs shown in Supplementary Fig. 3. E. MHCII-IA.[b]-KLVFFAEDVGSNKGA (Aβ T cell epitope) tetramer binding confirming the Aβ reactivity of engineered $TCR_{A\beta}$-Tregs incubated with Aβ-tetramer (blue) compared to $TCR_{A\beta}$-Tregs incubated with control-tetramer (orange) or polyclonal Tregs incubated with Aβ-Tetramer (red)

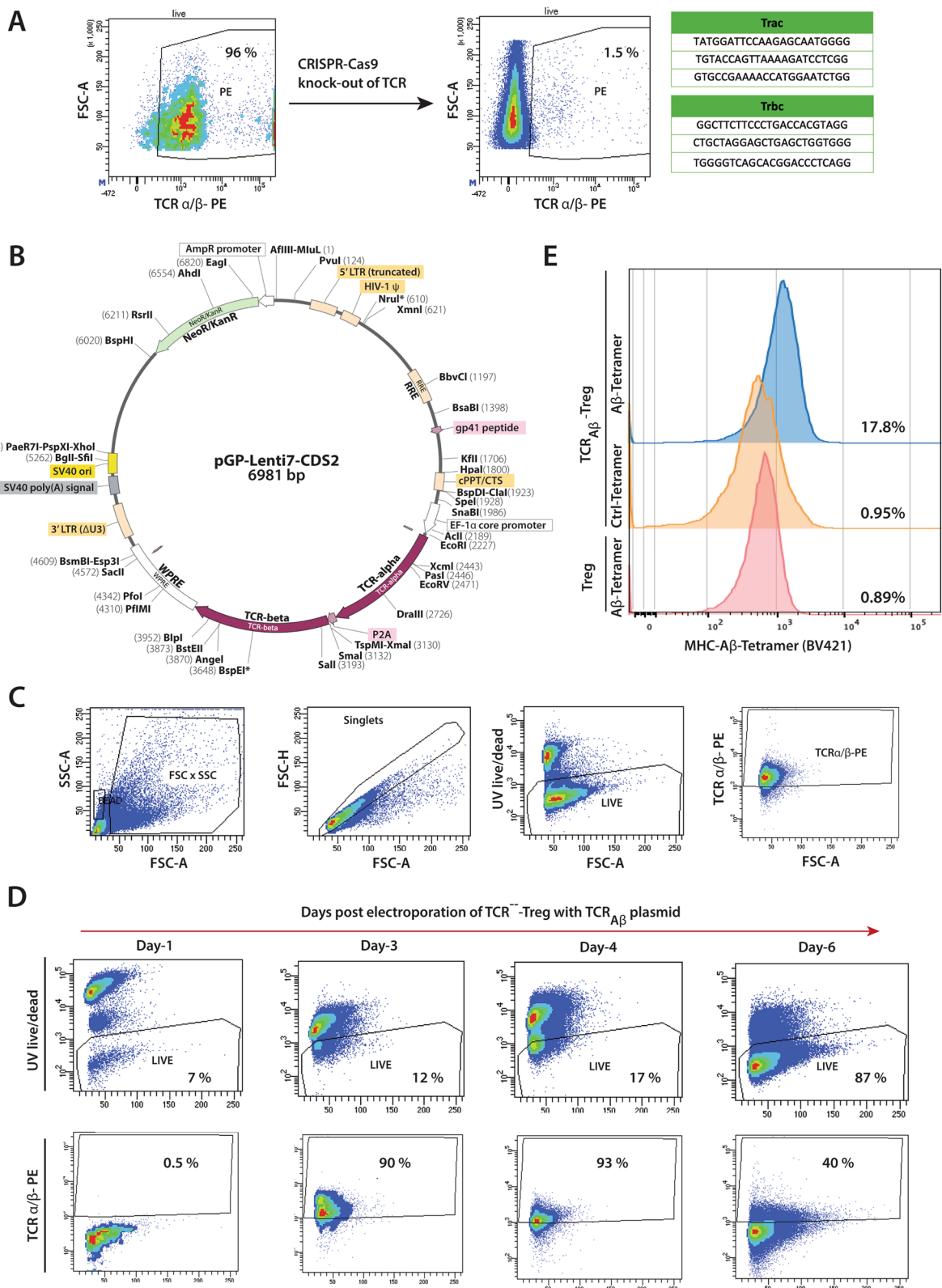Yeapuri *et al. Molecular Neurodegeneration*   (2023) 18:97

Page 8 of 22

Fig. 1 (See legend on previous page.)

responder (Tresp) cells. The Tresp suppressive function of Aβ-Treg was evaluated by co-incubating them with CSFE-labeled Tresp cells in the presence of Dynabeads (mouse T-cell activator CD3/CD28). Knocking out the TCR (TCR^{--}-Tregs) showed a non-significant reduction in ability to suppress Tresp cell proliferation compared to polyclonal Treg (Fig. 2B). TCR$_{Aβ}$-Tregs showed a significant increase in the ability to suppress Tresp cell proliferation compared to polyclonal Tregs (Fig. 2A,B). The increase in suppressive function was dose-dependent on the amount of TCR$_{Aβ}$ plasmid electroporated. The TCR$_{Aβ}$-Tregs that received 0.50 μL of TCR$_{Aβ}$ plasmid showed higher suppressive function compared to those that received 0.25 μL of the plasmid. To further confirm the Aβ-specific Treg suppressive function, a modified Treg function assay was performed where CFSE-labeled Tresps were pre-stimulated with Dynabeads overnight, the beads removed, and the stimulated Tresps co-cultured with TCR$_{Aβ}$-Tregs for three days in the presence of Aβ-tetramer alone as stimulant. Polyclonal Tregs showed similar suppression of Teff cells as compared to TCR^{--}-Treg (Fig. 2D,E). TCR$_{Aβ}$-Tregs showed a significant increase in Aβ-tetramer-dependent Teff suppressive function compared to polyclonal Tregs (Fig. 2D,E). Further, we looked at the cytokine profile of the engineered TCR$_{Aβ}$-Tregs stimulated with PMA and ionomycin using a mouse cytokine array kit. Compared to polyclonal Tregs, TCR$_{Aβ}$-Tregs produced increased Th2-polarizing cytokines (Fig. 2C, Supplementary Table 1). Further, TCR$_{Aβ}$-Tregs showed increased secretion of IL-4 which supports diminished production of IFN-γ. Further chemokines CCL2 and CCL5 that are involved in Treg recruitment in vivo were also elevated (Fig. 2C, Supplementary Table 1).

Adoptive transfer of TCR$_{Aβ}$-Tregs improves memory formation.

We previously showed that adoptive transfer of 1×10^6 monoclonal Aβ-specific Teff clones accelerates memory impairment [41]. As the TCR$_{Aβ}$-Tregs generated via electroporation only transiently express TCR$_{Aβ}$, but are functionally capable, we adoptively transferred 1×10^6 cells once a week, for 3 weeks and evaluated the mice for spatial learning and memory in both the radial arm water maze (RAWM) and Y maze test. These tests were performed a day after the final adoptive cell transfer. In the Y maze test, the APP/PS1 mice demonstrated memory impairment with a significant ($p < 0.01$) reduction in number of arm entries compared to non-transgenic mice. Only APP/PS1 mice treated with TCR$_{Aβ}$-Tregs showed increased number of arm entries. While number of entries did not reach significance compared to untreated APP/PS1 mice, they were not statistically different from those of non-Tg mice compared against Treg or EV-Treg treated APP/PS1 mice (Fig. 3A, B). APP/PS1 mice treated with polyclonal Tregs or EV-Tregs (TCR^{--}-Treg electroporated with empty plasmid vector) were not different from untreated APP/PS1 mice in tested memory outcomes.

In the RAWM test, the APP/PS1 mice showed signs of memory impairment as evidenced by significant increases in the numbers of errors in late retention trial T5 ($p < 0.05$ in block-1 and $p < 0.001$ in block-3) compared to non-transgenic mice (Fig. 3C). Notably, treatment of APP/PS1 with TCR$_{Aβ}$-Tregs showed significant improvement in memory outcomes as demonstrated by significantly reduced errors in late retention trial T5 ($p < 0.05$ in block 1 and $p < 0.01$ in block 3) compared to untreated APP/PS1 mice. APP/PS1 mice treated with either polyclonal Tregs or control EV-Tregs did not show

(See figure on next page.)

Fig. 2 *Characterization of TCR$_{Aβ}$-Treg immunosuppressive function.* **A**. Representative histograms of Treg suppressive function assay. CFSE-labelled-Tresp (CD4+ CD25-) cells co-incubated (3 days) with decreasing ratio of Treg:Tresp cells in the presence of anti-CD3/CD28 Dynabeads. Undivided CFSE+Tresp (green peaks), divided CFSE+Tresp (red peaks), Treg cells (blue peaks). **B**. Quantitation of the immunosuppressive function of TCR$_{Aβ}$-Tregs generated by electroporation of TCR^{--}-Tregs (TCR knockout Tregs) with 0.25 μL or 0.5 μL of TCR$_{Aβ}$ plasmid (plasmid conc. = 1.5 μg/ μL). Engineered TCR$_{Aβ}$-Tregs, Tregs or TCR knockout Treg (TCR^{--}-Tregs) were co-cultured with CFSE+Tresp cells (50 K cells/well) from non-Tg mice in the presence of anti-CD3/CD28 Dynabeads. Treg mediated immune suppression (%Inhibition) = [1- (% proliferation of Tresp:Treg dilution ÷ % proliferation of stimulated Tresp alone)] × 100. Linear regression analysis indicates $r^2 > 0.90$, $p < 0.03$ for TCR^{--}-Tregs electroporated with 0.25 μL or 0.5 μL of TCR$_{Aβ}$ plasmid. Regression of polyclonal Tregs were $r^2 > 0.50$, $p < 0.03$. Table contains *p*-values for slopes and intercepts of Treg functions compared by linear regression analysis, $n = 3$. Data presented as mean ± SEM **C**. Supernatants of Treg (polyclonal), TCR^{--}-Tregs (TCR knockout Tregs), and TCR$_{Aβ}$-Tregs (TCR^{--}-Tregs + 0.5 μL TCR$_{Aβ}$ plasmid) stimulated with PMA/ionomycin assessed by mouse cytokine array. Data represents mean intensities and statistical differences determined by two-way ANOVA tabulated in Supplementary Table 1. D. Quantification of Aβ-mediated Treg suppressive function. CFSE+Tresp cells from non-Tg mice were stimulated overnight with anti-CD3/CD28 Dynabeads. Pre-stimulated CFSE+Tresps were co-cultured with TCR$_{Aβ}$-Tregs (TCR^{--}-Tregs + 0.5 μL TCR$_{Aβ}$) or Tregs (polyclonal) or TCR knockout Treg (TCR^{--}-Tregs) at 1:1 ratio (50,000 cells/well) for 3 days with only MHC-Aβ-tetramer or control-tetramer. Treg–mediated % inhibition was calculated, and statistical differences were determined by one-way ANOVA followed by Turkey's post hoc test. ***$p < 0.001$, $n = 3$. Data presented as mean ± SEM **E**. Representative histograms of Aβ-mediated Treg suppressive function of engineered Tregs co-incubated with pre-stimulated CFSE+Tresp cells in the presence of Aβ-tetramer or control-tetramer. Undivided CFSE+Tresp (green peaks), divided CFSE+Tresp (red peaks), Treg cells (blue peaks)
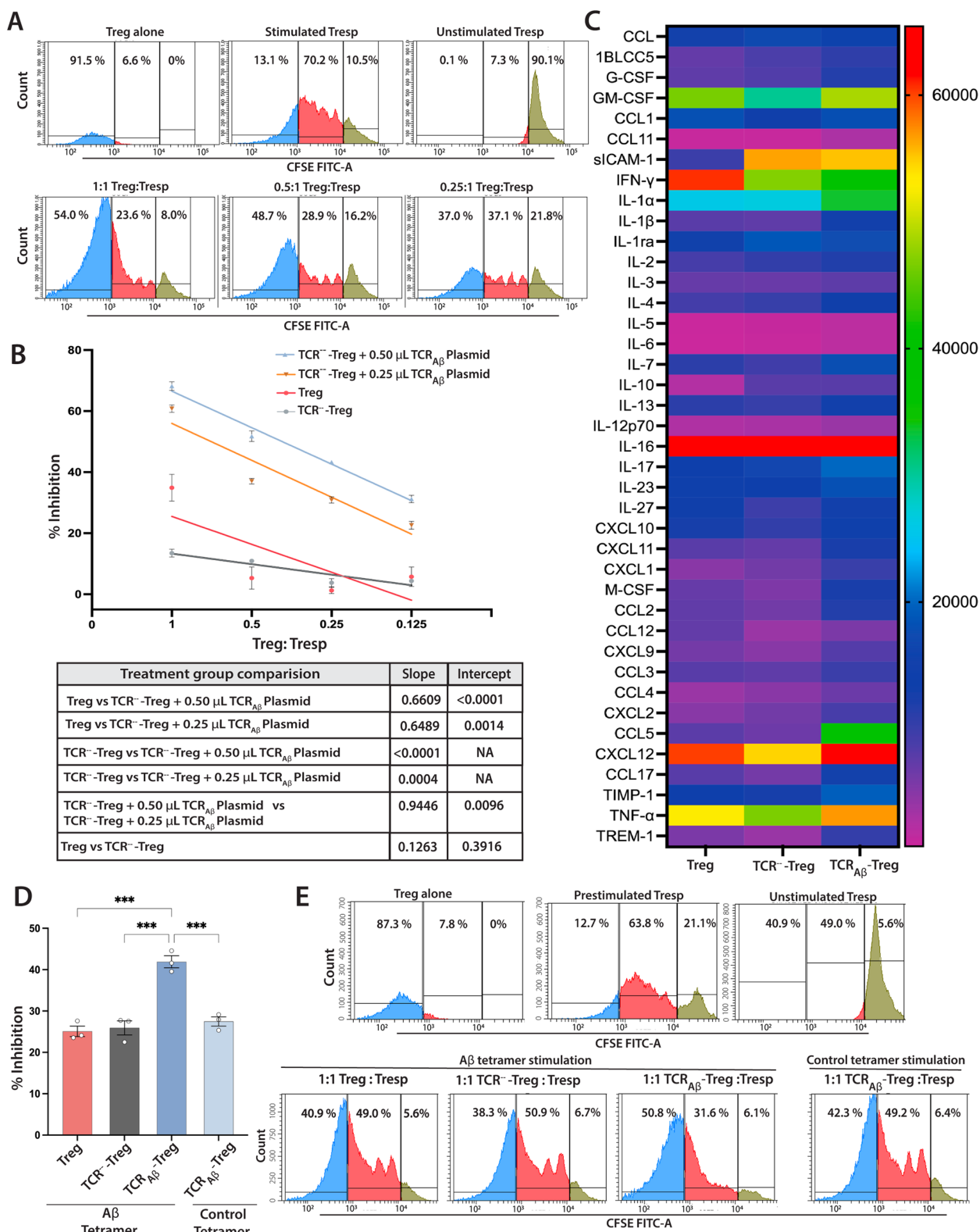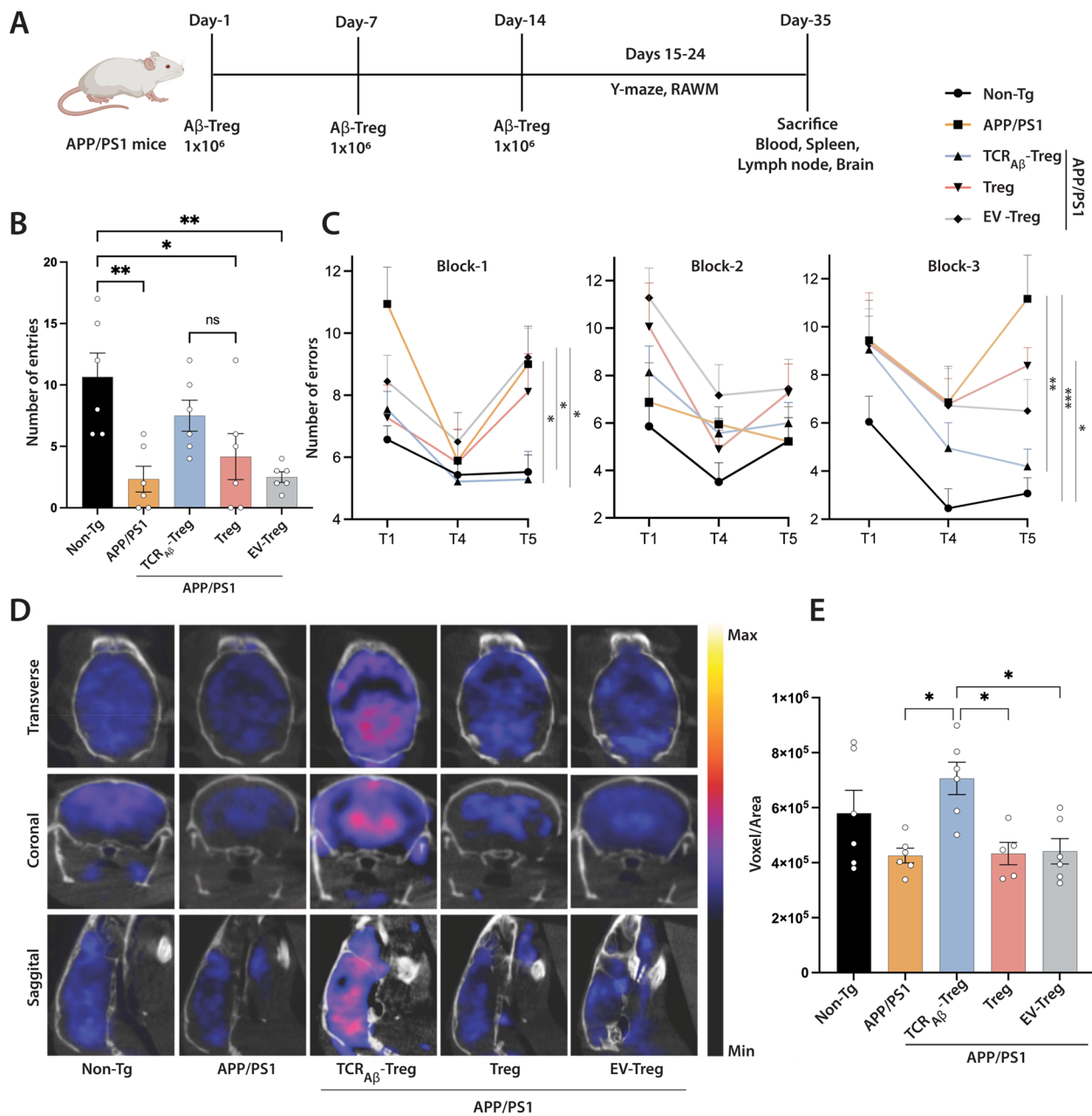
Fig. 2 (See legend on previous page.)

Fig. 3 *Adoptive transfer of TCR$_{A\beta}$-Tregs improve memory function in APP/PS1 mice*. A. Experimental timeline of adoptive transfer experiments. Eight-month-old non-Tg mice ($n=6$) were untreated, and age-matched APP/PS1 mice were untreated or treated with 1×10^6 TCR$_{A\beta}$-Tregs, polyclonal Tregs (Treg), or EV-Tregs (TCR^{--}-Tregs electroporated with empty plasmid vector). **B** Y maze test performed on experimental mice after adoptive transfers to evaluate spontaneous alteration in mice freely exploring each arm of the Y maze over eight minutes. Successful entries were defined as consecutive entries into three different arms and the number of entries/mice were recorded ($n=6$). **C.** Radial arm water maze (RAWM) test performed with experimental mice after adoptive transfers. After four trials (T1-T4) the mice were returned their cages for 30 min and reintroduced into the T4 arm for the delayed retention trial (T5). Each trial lasted for 1 min and errors were scored when the mice entered the wrong arm or entered the arm without climbing the platform or didn't make a choice for 20 s. The trial ended when the mice climbed and stayed on platform for at least 10 s. Errors of 9-day trial were divided into three blocks: Block-1 (days 1–3), Block-2 (days 4–6), Block-3 (days 7–9). The errors in each block were averaged for statistical analysis ($n=6$). **D** Representative ^{18}F-FDG PET images of brain glucose uptake in different treatment groups on the day of sacrifice. **E** Quantification of ^{18}F-FDG PET brain glucose uptake on the day of sacrifice ($n=5$—6). **B**, **C**, and **E** Data presented as mean ± SEM. One-way ANOVA followed by Turkey's post hoc test was used to determine significant differences between experimental groups. *$p<0.05$, **$p<0.01$, ***$p<0.001$

any improvement in memory outcomes in the RAWM test. Overall, the results demonstrate that treatment with amyloid β-specific TCR$_{Aβ}$-Tregs improves memory outcomes in APP/PS1 mice compared to treatment with polyclonal Tregs.

Brain glucose hypometabolism is a prominent feature of AD. Improvement in brain glucose uptake and metabolism is a biomarker for memory improvement [49, 50]. ^{18}F-FDG PET imaging is commonly used for the diagnosis of dementia states in AD patients and in preclinical animal models [52, 53]. Compared to non-transgenic mice, APP/PS1 mice showed reduced brain glucose uptake (Fig. 3D and E). Treatment of APP/PS1 mice with TCR$_{Aβ}$-Tregs showed significant increase ($p < 0.05$) in glucose uptake compared to APP/PS1 mice that were untreated or treated with polyclonal Tregs or EV-Tregs. Treatment with either polyclonal Tregs or EV-Tregs did not show significant improvement in brain glucose uptake compared to untreated APP/PS1 mice. Together, increased brain glucose uptake after treatment with TCR$_{Aβ}$-Tregs parallels the improved memory outcomes in the Y maze and RAWM tests.

TCR$_{Aβ}$-Tregs facilitate Treg homing to the brain.

Our central hypothesis is that given the Aβ reactivity of engineered Tregs, those Tregs will migrate to and accumulate in amyloid rich brain regions. These cells would then generate neuroprotective anti-inflammatory outcomes. Initially to evaluate this, we assessed the distribution of total Tregs (CD4+CD25+FoxP3+) by flow cytometry (Fig. 4A) in the spleen, lymph nodes, blood, and brain of WT mice, untreated APP/PS1 mice, or APP/PS1 mice recipients treated with TCR$_{Aβ}$-, polyclonal-, or EV-Treg. Mice were sacrificed 2 weeks after the final adoptive transfer. No significant differences in the frequencies of total Tregs were detected in the spleens and lymph nodes in each of the treatment groups (Fig. 4B). In the blood, compared to non-transgenic mice, untreated APP/PS1 mice showed reduced, but not significant, total

Treg frequencies. Notably, APP/PS1 mice treated with polyclonal Tregs showed significantly increased frequencies of total Tregs compared to untreated APP/PS1 mice. However, APP/PS1 mice treated with TCR$_{Aβ}$- or EV-Tregs showed no significant differences in total Treg frequencies. Interestingly, total Tregs in the brain showed a significant increase in APP/PS1 mice treated with TCR$_{Aβ}$-Tregs as compared to all treatment groups. Moreover, mice treated with control EV-Tregs showed significant reduction of total Tregs compared to all groups. Taken together, treatment with TCR$_{Aβ}$-, polyclonal-, or EV-Tregs showed little or no effect on the distribution of total Tregs in the spleen, lymph node, and blood suggesting most Tregs remain predominantly in the systemic circulation, whereas treatment with TCR$_{Aβ}$-Tregs owing to their Aβ reactivity, easily infiltrate the brain as it is a major site of pathological amyloid deposition and neuroinflammation.

To further confirm the brain-targeting efficacy of engineered Tregs, we adoptively transferred ^{18}F-FDG radiolabeled wild-type polyclonal Tregs or TCR$_{Aβ}$-Tregs to APP/PS1 mice and evaluated their biodistribution by PET imaging at 0.5, 2, 4, and 6 h after transfer. Interestingly, compared to wild-type Tregs, TCR$_{Aβ}$-Tregs yielded significantly higher signal in the brain 0.5-h post-transfer (Fig. 4C and D). Increased TCR$_{Aβ}$-Treg infiltration into the brain was sustained for up to 4–6 h. Together, this data highlights more efficient brain-targeting of TCR$_{Aβ}$-Tregs compared to polyclonal Tregs.

TCR$_{Aβ}$-Tregs and systemic immune function

Tregs play a major role in maintaining immune tolerance and Treg dysfunction has been implicated in progression of AD pathology [29, 54, 55]. Studies have shown a protective role of ex vivo expanded Tregs in AD [28, 29, 56]. Herein, we evaluated changes in the suppressive function of peripheral Tregs after adoptive transfer of TCR$_{Aβ}$-, polyclonal-, or EV-Tregs to APP/PS1 recipients. Compared to Tregs from untreated APP/PS1 mice, Tregs from

(See figure on next page.)

Fig. 4 *Adoptive transfer of TCR$_{Aβ}$-Tregs increase Treg homing to brain and Treg function.* **A** Representative flow cytometric gating strategy for quantification of total Treg frequencies (CD4+CD25+FoxP3+). **B** Frequencies of Tregs in spleen, lymph node, blood, and brain in APP/PS1 mice adoptively transferred with three, weekly doses of 1×10^6 TCR$_{Aβ}$-Tregs, polyclonal Tregs (Treg) or EV-Tregs (TCR^{--}-Tregs electroporated with empty plasmid vector) ($n = 5$-6) **C** Representative PET images of APP/PS1 brains after adoptive transfer of ^{18}F-FDG radiolabeled polyclonal Tregs (Treg) or TCR$_{Aβ}$-Tregs and their biodistribution evaluated at 0.5, 2, and 6 h. **D** Quantitation of radioactivity from PET images of ^{18}F-FDG radiolabeled Tregs or TCR$_{Aβ}$-Tregs in the brain acquired at 0.5, 2, 4, and 6 h ($n = 3$). **E** Suppressive capability of peripheral Tregs from APP/PS1 mice that were untreated or treated with TCR$_{Aβ}$-Tregs, polyclonal Tregs (Treg) or EV-Tregs (TCR^{--} -Tregs electroporated with empty plasmid vector). Linear regression analysis indicates r.^{2} > 0.90, $p < 0.001$ for all treatment groups. Table contains p-values for slopes and intercepts of compared linear regression analysis ($n = 3$). Flow cytometric analysis of; **F** MHC-Aβ-tetramer positive Tregs (CD4+CD25+Aβ-Tetramer+) and **G** MHC-Aβ-tetramer positive CD4+CD25-Aβ-Tetramer+splenocytes stimulated with Aβ protein and low dose IL-2, ($n = 5$–6). **B**, **F** Data presented as mean ± SEM. One-way ANOVA followed by Turkey's post hoc test was used to determine significant differences between experimental groups. *$*p < 0.05$, $**p < 0.01$, $***p < 0.001$, $****p < 0.0001$*
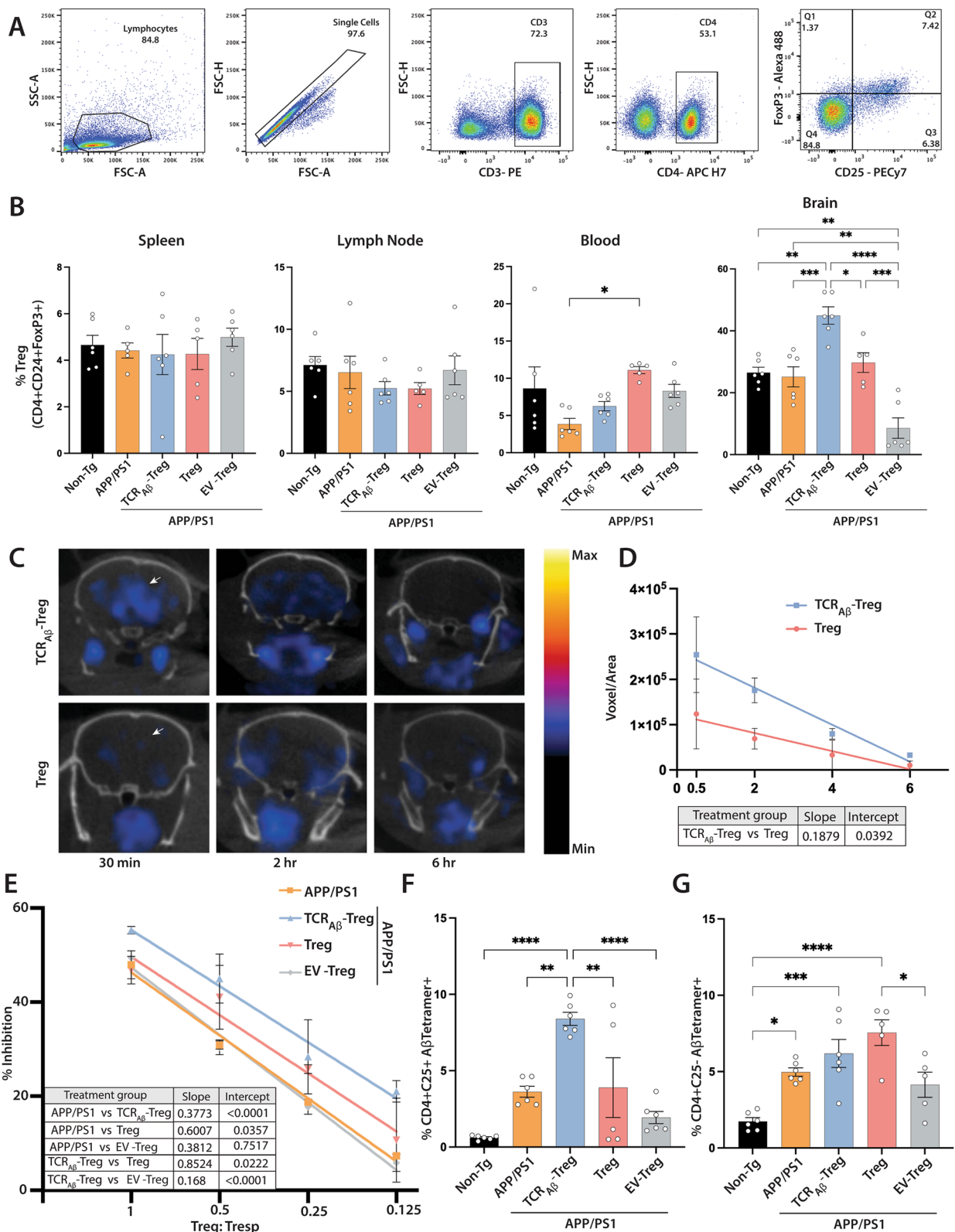
Fig. 4 (See legend on previous page.)

APP/PS1 mice treated with TCR$_{A\beta}$-Tregs or polyclonal Tregs showed elevated suppressive function with TCR$_{A\beta}$-Tregs inducing the highest suppression (Fig. 4E). In contrast, Tregs from mice receiving EV-Tregs were functionally like untreated APP/PS1 mice.

Further, given the transient nature of TCR$_{A\beta}$ expression by TCR$_{A\beta}$-Tregs, we examined TCR$_{A\beta}$ expression after adoptive transfer TCR$_{A\beta}$-, polyclonal-, or EV-Tregs to APP/PS1 recipient animals. To perform these evaluations, splenocytes isolated at the time of sacrifice 2 weeks after the last transfer were stimulated with Aβ_{42} peptide in the presence of feeder cells (irradiated splenocytes 1:5 ratio) and low dose IL-2 (20U/mL) for a week. Post-stimulation, cells were stained with fluorescently labeled Aβ-tetramer (MHCII-IA^b–KLVFFAEDVG-SNKGA) to evaluate the frequency of TCR$_{A\beta}$-reactive CD4+CD25+ Tregs. As expected, due to the presence of amyloid-β deposits in the AD mouse model, TCR$_{A\beta}$ reactive Tregs were observed in untreated APP/PS1 mice at higher levels than found in non-transgenic mice. (Fig. 4F). However, only APP/PS1 mice treated with TCR$_{A\beta}$-Tregs showed significant increase in the frequency of Aβ tetramer reactive Tregs (CD4+CD25+) compared to untreated APP/PS1 mice or mice treated with polyclonal Tregs or EV-Tregs. Treatment of APP/PS1 mice with polyclonal Tregs or EV-Tregs induced no significant increases in frequencies of Aβ tetramer reactive Tregs. Additionally, there was no significant changes in Aβ tetramer reactive CD4+CD25- cell populations in all treatments compared against APP/PS1 mice.

TCR$_{A\beta}$-Tregs reduce the amyloid burden

We next evaluated the effect of TCR$_{A\beta}$-Tregs on the amyloid burden in cortex and hippocampus of AD mice. While APP/PS1 mice show significant amyloid deposits and loads, adoptive transfer of TCR$_{A\beta}$-Tregs reduced both soluble and insoluble fragments of Aβ in the cortex, whereas polyclonal Treg treatment slightly, but insignificantly, reduced Aβ deposition (Fig. 5A). Treatment with EV-Tregs did not significantly affect amyloid load compared to untreated APP/PS1 mice. We then evaluated Treg-mediated effects on amyloid plaque deposition in the mice brain by immunohistochemistry. Treatment with TCR$_{A\beta}$-Tregs reduced amyloid plaque in the cortex compared to untreated APP/PS1 mice and adoptive transfer of TCR$_{A\beta}$-Tregs or polyclonal Tregs reduced total Aβ plaques in hippocampal tissues as determined by pan-Aβ staining (Fig. 5B and D). Treatment with EV-Tregs showed no significant effects in either cortex or hippocampus. We next determined the effects of Tregs on brain area occupied by dense amyloid plaques using Thioflavin-S immunohistochemistry. Adoptive transfer of either TCR$_{A\beta}$-Tregs or polyclonal Tregs to APP/PS1 mice

reduced dense amyloid plaque deposition in both the cortex and hippocampus compared with untreated APP/PS1 mice (Fig. 5C and D). Treatment with EV-Tregs did not show significant differences in cortical or hippocampal tissues compared to those tissues of APP/PS1 mice.

TCR$_{A\beta}$-Tregs reduce reactive microglia

Microglia activation is a common hallmark of neuroinflammation observed in AD patients and animal models [57]. To determine the effects of TCR$_{A\beta}$-Tregs on reactive microglial responses, we counted Iba-1-reactive cells with amoeboid morphology in cortex and hippocampus after adoptive transfer of TCR$_{A\beta}$-, polyclonal-, or EV-Tregs to APP/PS1 recipients. Immunohistochemistry visually showed a remarkable increase in the number Iba1 positive (Iba1+) amoeboid cells in cortical and hippocampal tissues of untreated APP/PS1 mice compared to non-transgenic mice suggesting increased microglia activation in AD mice (Fig. 6A). Compared with untreated AD mice, treatment with TCR$_{A\beta}$-Tregs or polyclonal Tregs reduced numbers of Iba1+reactive microglia in cortices and hippocampi of APP/PS1 AD mice with greater reductions in cortical tissues produced by TCR$_{A\beta}$-Tregs (Fig. 6A and B). Treatment with EV-Tregs yielded no significant reductions of reactive microglia numbers in either the hippocampus or the cortex of APP/PS1 mice. To further characterize the microglial signature after TCR$_{A\beta}$-Treg treatment, we evaluated the transcriptional changes in disease-associated microglia (DAM) markers such as Clec7A, Itgax and TREM2 [58]. In line with the reduced reactive microglial phenotype, we observed decreased TREM2 expression with both polyclonal Treg and TCR$_{A\beta}$-Treg treatments (Fig. 6C). However, only TCR$_{A\beta}$-Treg treatments reached significance compared against both untreated and EV-Treg treated APP/PS1 mice. Additionally, trends in Clec7A and Itgax expressions were recorded but without significant changes seen following TCR$_{A\beta}$-Treg treatments (Fig. 6C). In addition to microglia, astrocytes have been implicated in promoting neuroinflammation in Alzheimer's disease [59, 60]. Reactive astrocytes were assessed by evaluating GFAP expression. Both Treg and TCR$_{A\beta}$-Treg treatments showed significantly reduced GFAP expression. However, only TCR$_{A\beta}$-Treg treatments show the highest reductions compared to untreated and EV-Treg treated APP/PS1 mice (Fig. 6C).

Discussion

We posit that Aβ-specific Tregs (TCR$_{A\beta}$-Treg) can be a disease modifying therapy for AD. In this study, we compared the neuroprotective efficacy of TCR$_{A\beta}$-Treg against polyclonal Treg as a treatment strategy in the APP/PS1 mouse model for AD. The Aβ-Treg cells were engineered
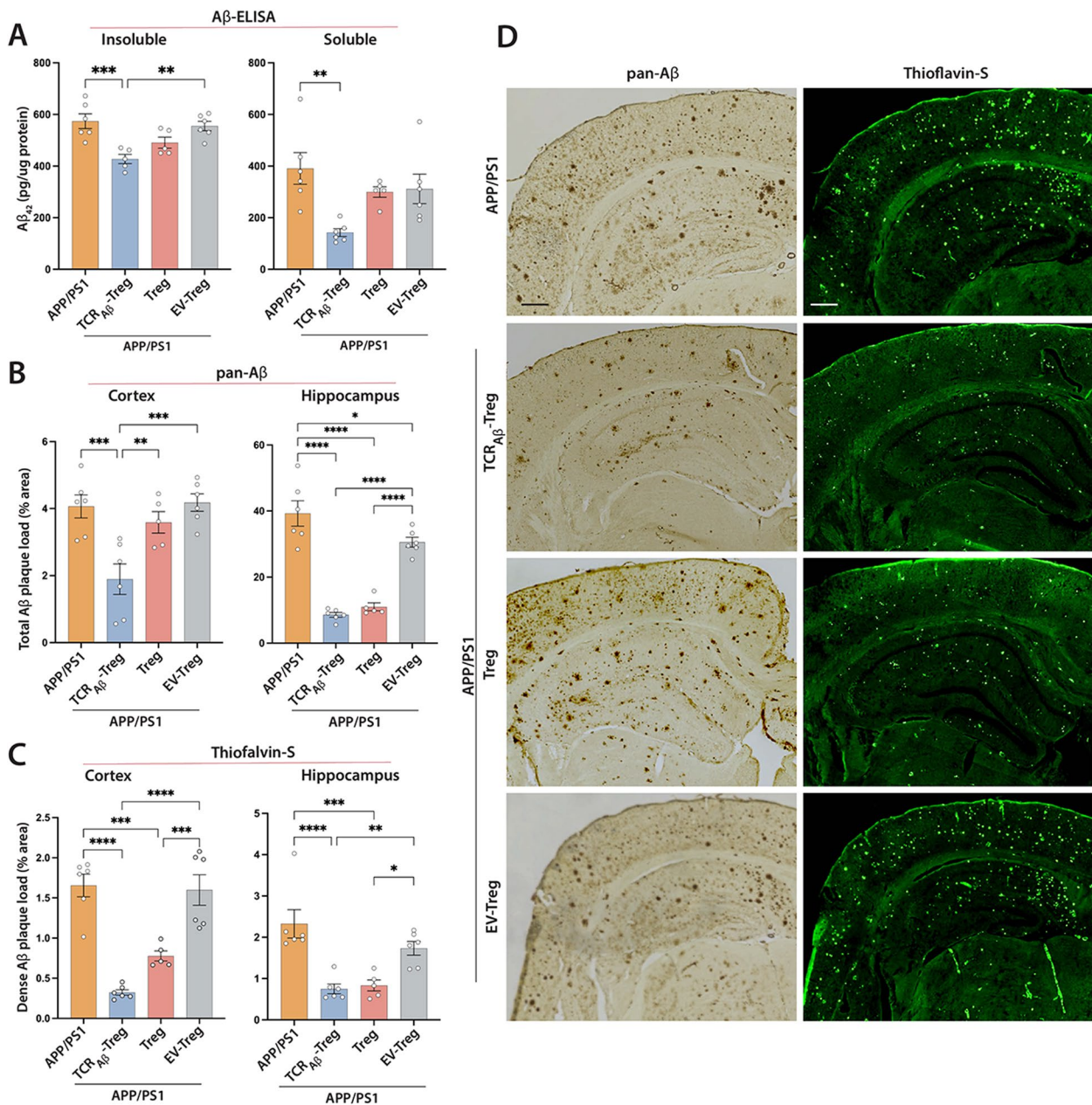
Yeapuri *et al. Molecular Neurodegeneration*   (2023) 18:97

Page 15 of 22

Fig. 5 *Adoptive transfer of TCR$_{A\beta}$-Tregs reduces amyloid load in APP/PS1 mice*. APP/PS1 mice were untreated or treated with TCR$_{A\beta}$-Tregs, polyclonal Tregs (Treg) or EV-Tregs (TCR^{--}-Tregs electroporated with empty plasmid vector) by adoptive transfer and brain tissues acquired 3 weeks post adoptive transfer **A**. ELISA performed to quantify Aβ_{1-42} levels in the brain using Tris–HCl (soluble) and guanidine-HCL (insoluble) fractions of cortical tissue. **B**, **C**. ImmunohistoFchemistry (pan-Aβ) and immunofluorescence (Thioflavin-S) to determine the area occupied by insoluble Aβ plaques in cortical and hippocampal regions. **D** Representative images showing amyloid plaque (pan-Aβ) and Thioflavin-S staining in different brain regions. Percent area occupied was quantified using Cavalieri estimator probe. Scale bar = 100 µm. **A-C** Data presented as mean ± SEM for $n = 5$–6 mice/group. One-way ANOVA followed by Turkey's post hoc test was used to determine significant differences between experimental groups. *$p < 0.05$, **$p < 0.01$, ***$p < 0.001$, ****$p < 0.0001$

using the TCR$_{A\beta}$ identified from Aβ-reactive monoclonal Teff cells [41]. The antigen specificity was shown to enhance Treg-mediated neuroprotective responses. Comparisons between TCR$_{A\beta}$-Tregs and polyclonal Tregs demonstrated improved neuroprotective responses which were defined by reduction of reactive microglia, diminished amyloid deposition, and improved memory formation. Notably, compared to the diffuse systemic

distribution of polyclonal Tregs, TCR$_{A\beta}$-Tregs specifically accumulated into the brain and elicit anti-inflammatory responses. The TCR$_{A\beta}$-Tregs exerted anti-inflammatory activities by both bystander and antigen-mediated immunosuppressive activities.

These results fulfil an unmet need as recent FDA-approved antibody therapies for AD have met with mixed success [61]. This allows an increased interest in developing T-cell therapies for AD. Notably, prior studies have identified both CD4 + and CD8 + T cell subsets with either pro-inflammatory or regulatory activities which have yielded mixed disease outcomes for neurodegenerative disorders. While the CD4 + T cell subsets have well defined cell surface markers, transcription factors, and cytokines to categorize them into subtypes such as Th1, Th17, and Treg; the CD8 + T cell effects on disease remains poorly defined [62]. Prior reports demonstrated an AD immune signature of increased numbers of CD8 + T effector memory CD45RA + (T$_{EMRA}$) cells negatively associated with cognition and single-cell RNA sequencing showed their effect on TCR signaling [22, 62, 63]. In contrast works from our own laboratory have demonstrated a functional role for CD4 + Tregs in the control of neuroinflammation and affecting neuronal repair [37, 38, 40]. CD4 + CD25 + Foxp3 + Tregs have been shown to control Teff immune responses through restraint of T cell activation. This leads to the maintenance of brain tissue homeostasis and repair and shown to be effective in a broad range of neurodegenerative diseases that include amyotrophic lateral sclerosis, stroke, PD, and AD [28, 35–40]. Brain-resident CD69 + Tregs are present in the healthy brain with rapid expansion observed during neuroinflammatory processes serving to control astrogliosis by amphiregulin and shifting microglia into neuroprotective signatures through IL-10 [64, 65]. Tregs, on the other hand, have been shown to have a beneficial role in preclinical mouse models of AD. Transient depletion of Tregs accelerate cognitive decline, whereas amplification of Tregs including the use of low dose IL-2 improve cognitive outcomes in the same APP/PS1 mice used in this report [36]. Further studies have shown that induction of Tregs using therapeutic agents

or adoptive transfer of polyclonal Tregs is neuroprotective outcomes against AD, PD [28, 36, 38, 39] and multiple sclerosis (MS) [66]. The safety and feasibility of a polyclonal Treg therapy have been established by numerous clinical trials in the field of autoimmune diseases and transplant rejection [67]. However, polyclonal Treg treatments rely on the bystander effect from Tregs homing into different tissues in an antigen-independent fashion resulting in global immune suppression [68]. Preclinical studies in autoimmune diseases indicate that antigen-specific Tregs could be more efficient by controlling pathological immune responses in a disease specific manner [69–73]. Antigen-specific Tregs migrate and accumulate at the site of cognate antigen expression where they exert both bystander and antigen-specific immune responses, and reduce complications associated with broad immunosuppression [69, 74]. This can be advantageous in AD where Treg access to diseased brain regions is required for neuroprotective and anti-inflammatory responses.

Identifying endogenous disease reactive Tregs or developing them though immunization is further complicated by low Treg precursor frequencies and lack of effective expansions. Recently, putative Aβ-reactive Tregs were generated by Aβ immunization of Treg depleted mice [31]. However, this approach however is limited by the fact that the Tregs generated are not monoclonal due to the low precursor frequencies of antigen reactive Treg post immunization [75]. Additionally, the lack of comparisons made against polyclonal Treg treatment in the study complicates the interpretation of the potential advantage of antigen specific Treg therapy. Current efforts at developing antigen-specific Tregs rely on transducing antigen-specific TCRs identified from Teff cells into Treg cells [76, 77]. Although, this approach was effectively used in manipulating human Treg cells, mouse Treg cells are extremely difficult to transduce [78]. Notably, our TCR$_{A\beta}$ lentiviral constructs while successfully transducing CEMSS, 3T3 and human PBMC's with the TCR$_{A\beta}$, were less effective at transducing mouse Tregs. To overcome this limitation, we generated TCR$_{A\beta}$-Tregs that transiently express an Aβ-specific TCR by electroporation of a plasmid encoding the TCR$_{A\beta}$. The rationale behind

(See figure on next page.)

Fig. 6 *Adoptive transfer of TCR$_{A\beta}$-Tregs reduces reactive microglia in APP/PS1 mice.* **A** APP/PS1 mice were untreated or treated with TCR$_{A\beta}$-Tregs, polyclonal Tregs (Treg) or EV-Tregs (TCR^{--}-Tregs electroporated with empty plasmid vector) by adoptive transfer and brain tissues acquired 3 weeks post-transfer. Untreated non-transgenic mice served as controls. Representative images showing Iba1 reactive cells in brain regions. Scale bar = 100 μm. Areas with most Iba1 + reactive microglia are highlighted by inserts for the cortex and hippocampus. Scale bar = 50 μm. **B** Number of Iba1 + reactive microglia were quantified from immunohistochemistry in cortex and hippocampus using Optical Fractionator probe of Stereo Investigator. Data presented as mean ± SEM for 5–6 mice per group. **C** Changes in the expression of the disease-associated genes for astrocytes (GFAP) and microglia (Clec7A, Itgax, and TREM2) in cortical tissue by qPCR. Obtained CT values were normalized against the RPLP0 gene and non-Tg mice was used as control. Data presented as mean ± SEM. One-way ANOVA followed by Turkey's post hoc test was used to determine significant differences between experimental groups. *$p < 0.05$, **$p < 0.01$, ***$p < 0.001$, ****$p < 0.0001$
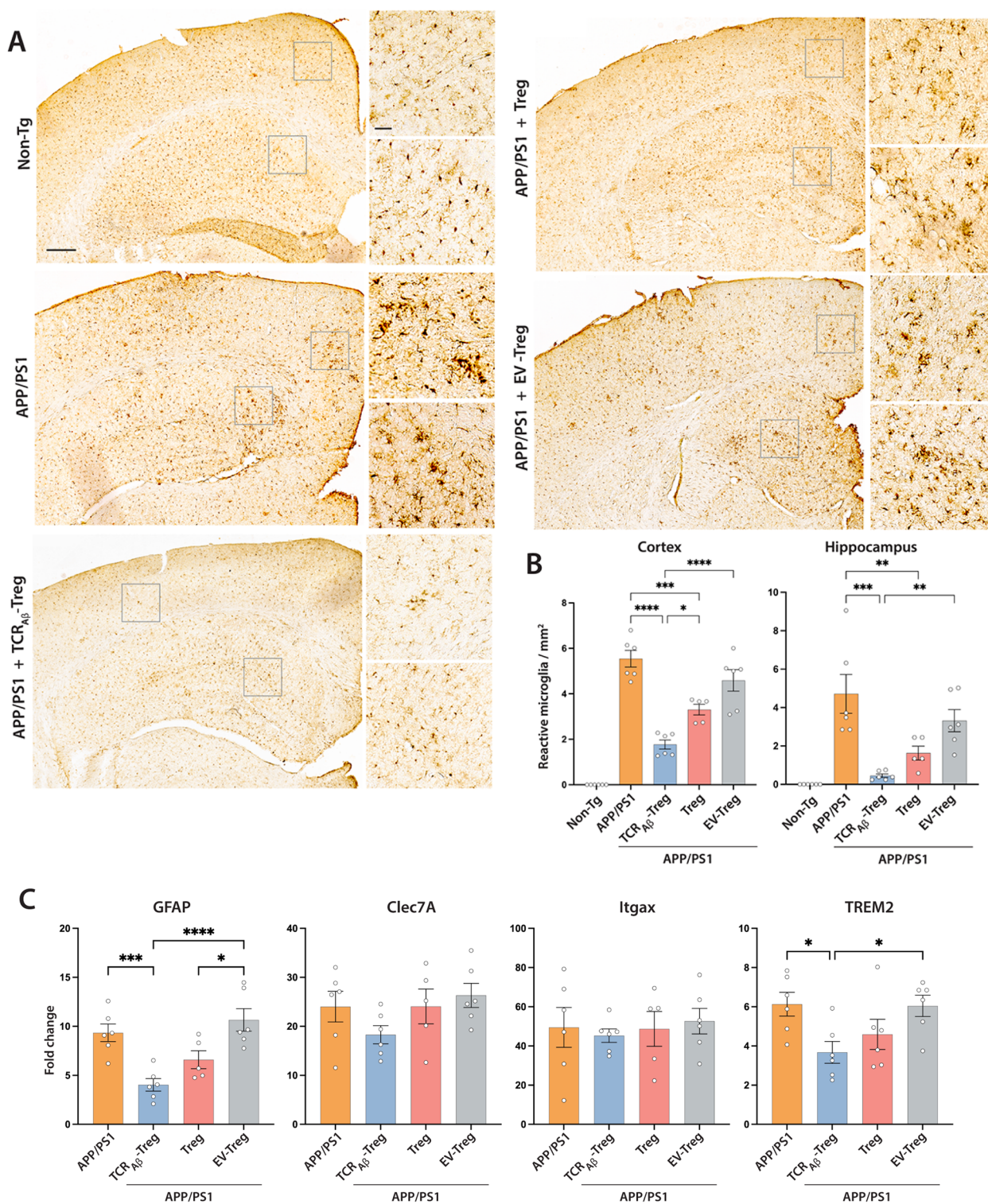
Fig. 6 (See legend on previous page.)

this approach is that in a therapeutic setting, adoptively transferred Tregs need not persist indefinitely, but long enough to confer suppressive capacity to other immune cells located at the affected tissue via a phenomenon called 'infectious tolerance' [79, 80]. Therefore, Treg cells transiently expressing $TCR_{A\beta}$ will generate the necessary

Yeapuri *et al. Molecular Neurodegeneration*   (2023) 18:97

Page 18 of 22

proof-of-concept response for developing human TCR$_{A\beta}$-Tregs for therapeutic evaluation.

In the current study, monoclonal TCR$_{A\beta}$-Treg were generated by incorporating the Aβ-specific TCR identified from a highly reactive monoclonal Aβ-Teff cell previously developed in our lab [41]. Splenic Tregs were isolated from mice with homozygous MHC background (B6;129) and endogenous TCRs were eliminated using CRISPR-Cas9 technology to avoid nonspecific immune reactions. Electroporation of the plasmid encoding TCR$_{A\beta}$ generated antigen-specific Tregs that transiently expressed the Aβ-specific TCR. Aβ-specificity of the engineered TCR$_{A\beta}$-Tregs was demonstrated by recognition by an MHC-Aβ-peptide tetramer. TCR$_{A\beta}$-Tregs showed significantly higher immune suppression owing to the transfer of highly reactive TCR$_{A\beta}$. However, Tregs can show dominant bystander effect, where they suppress Teffs in an antigen non-specific manner [81]. Aβ-specific immunosuppressive function of the engineered TCR$_{A\beta}$-Tregs was shown when MHC-Aβ-tetramer was used as the Treg stimulant. Further evaluation of the cytokine profile shows that compared to polyclonal Tregs, TCR$_{A\beta}$-Tregs expressed decreased proinflammatory cytokines such as IFN-γ [28] and increased granulocyte–macrophage colony-stimulating factor (GM-CSF). This serves to support their abilities to elicit Treg differentiation from naïve T cells by tolerogenic dendritic cells which serve to polarize T cells toward Th2 phenotypes [82]. Additionally, increased production of IL-4 supports TCR$_{A\beta}$-Treg immunosuppressive functions of IFN-γ secreting CD4+ T cells [83] while CCL2 and CCL5 are potential chemokines in Treg recruitment in vivo [84]. Our data suggests that incorporating the TCR identified by disease-reactive Teffs is a viable strategy for engineering antigen-specific Tregs that are immunosuppressive in an antigen driven manner.

In a healthy brain, infiltration of peripheral lymphocytes is well-controlled [85]. However, with AD progression, the Aβ lymphatic drainage is compromised and leads to increased infiltration of peripheral immune cells that exacerbate AD pathology [85]. The central hypothesis behind developing antigen-specific Treg therapies for AD is to target Aβ-specific cells to amyloid-rich brain sites. In the current study, we show that in APP/PS1 mice, adoptively transferred TCR$_{A\beta}$-Tregs significantly infiltrate the brain, while transferred polyclonal Tregs predominantly remain in the peripheral circulation. ^{18}F-FDG radiolabeled cell tracking highlights the brain targeting efficacy of TCR$_{A\beta}$-Treg in an antigen-dependent manner. Although, TCR$_{A\beta}$-Tregs targeted the brain in APP/PS1 mice, they were able to significantly increase systemic Treg function owing to the high affinity TCR$_{A\beta}$ incorporated into the cells. Notably, even though the

engineered TCR$_{A\beta}$-Tregs only transiently expressed the Aβ-specific TCR, stimulation of Tregs with human-Aβ peptide showed higher MHC-Aβ-tetramer reactive Tregs in mice treated with TCR$_{A\beta}$-Tregs. These data suggested disease-specific priming of naïve Tregs. Cognitive function evaluated by ^{18}F-FDG PET is considered an imaging biomarker for AD [86–88]. Decreased ^{18}F-FDG uptake represents a reduction in neuronal energy demand mainly arising from synaptic loss caused by amyloid pathology in patients. Adoptive transfer of TCR$_{A\beta}$-Tregs also increased brain glucose uptake compared to treatment with polyclonal Tregs. Notably, increased brain glucose uptake after TCR$_{A\beta}$-Treg treatment correlated with improved memory outcomes in both RAWM and Y maze behavioral tests. Taken together, these results show that the TCR$_{A\beta}$-Tregs, even though transiently expressing the TCR$_{A\beta}$, were able to target the brain and improve brain function and memory outcomes.

Additionally, microglia serve a key role in processing and presenting self-antigens, including Aβ, to maintain immune tolerance [28, 89]. Non-activated microglia exhibit ramified morphology and can clear Aβ deposits through phagocytosis [45]. However, with disease progression microglia become more activated and acquire amoeboid morphology with compromised phagocytic capabilities and elevated neurotoxicity [35, 45]. Studies have shown that cerebral Tregs restrain microglial inflammatory responses, and treatment with ex vivo expanded polyclonal Tregs was shown to suppress microglial inflammation [30, 31, 90]. Our results show that TCR$_{A\beta}$-Tregs are more effective than polyclonal Tregs at reducing reactive microglia both in the cortex and hippocampus. The brain targeting capacity of TCR$_{A\beta}$-Tregs and subsequent increase in percentage of brain Tregs resulted in greater reduction in inflammatory phenotypes of microglia compared to polyclonal Treg treatment. In addition to transforming microglia to a non-reactive phenotype, our results show that TCR$_{A\beta}$-Tregs are more effective at reducing amyloid deposition in both hippocampal and cortical regions of the brain as demonstrated by reduced soluble and insoluble Aβ$_{1-42}$ load determined by ELISA and Aβ plaques quantitative IHC. Notably, compared to polyclonal Tregs, TCR$_{A\beta}$-Tregs were more effective at reducing dense, pathological Thioflavin-S positive Aβ deposits. Overall, our results show that the brain-targeting efficacy and disease-specific immunosuppressive function of TCR$_{A\beta}$-Tregs lead to improved reduction of neuroinflammatory reactive microglia which further enhance clearance of amyloid plaque.

In summary, the current findings demonstrate proof-of-concept preclinical data in which disease-specific TCR$_{A\beta}$-Tregs are more effective at reducing amyloid

pathology and improving cognitive outcomes than poly-clonal Tregs. The transient expression of $TCR_{A\beta}$ by engineered $TCR_{A\beta}$-Tregs is a noted limitation in the study. However, the strong neuroprotective results shown in APP/PS1 mice despite the transient expression of the $TCR_{A\beta}$ underlies the significant therapeutic potential achievable with 'long-lived' $TCR_{A\beta}$-Tregs. Notably, the results confirm a clinically translatable strategy to develop stably expressing human $TCR_{A\beta}$-Tregs. A second limitation is the absence of significant differences between $TCR_{A\beta}$-Tregs and Treg treatments on the hippocampal amyloid burden while significant reductions were recorded in the cortex. We posit that hippocampal quantitation is limited by the amounts of tissue regions available for testing. Taken together, the data support the hypothesis that TCRs engineered as chimeric antigen receptors (CARs) will enable further development of Treg therapies for AD.

Conclusion

This is a proof-of-concept study that confirms the feasibility of Aβ-specific Treg AD therapy. Treatment with $TCR_{A\beta}$-Tregs in a relevant animal model enabled reductions in reactive microglia, amyloid load, and cognitive decline. Importantly, $TCR_{A\beta}$-Tregs were demonstrated to target amyloid-rich regions in an AD-diseased brain while demonstrating antigen-specific immunosuppression. We conclude that Aβ-specific Tregs can be a translatable therapeutic approach for AD and perhaps other neurodegenerative diseases.

Abbreviations

AD	Alzheimer's disease
PD	Parkinson's disease
MS	Multiple Sclerosis
Aβ	Amyloid beta
TCR	T cell receptor
TCR^{--}-Treg	Endogenous TCR knocked out of Treg
$TCR_{A\beta}$-Treg	Aβ antigen specific Treg
EV-Treg	TCR^{--}-Treg electroporated with empty plasmid vector
Treg	T regulatory cell
Teff	T effector cell
Tresp	T responder cell
Iba-1	Ionized calcium binding adaptor molecule 1
^{18}F-FDG-PET	^{18}F-2-fluoro-deoxy- D-glucose positron emission tomography

Supplementary Information

The online version contains supplementary material available at https://doi.org/10.1186/s13024-023-00692-7.

> **Additional file 1.**

Author's information

Not Applicable.

Availability of data and materials

All data needed to evaluate the conclusions in the paper are included in the paper. The Aβ-TCR sequence used to engineer the Treg cells in the study is not publicly available due to the patent currently under review: Cell therapy for Alzheimer's disease" (EFS ID: 42,475,225, Application number: 63175747, Docket number: 21084P).

Declarations

Ethics approval and consent to particpate

The study was reviewed and approved by the animal welfare review board of the University of Nebraska Medical Center.

Consent for publication

Not applicable.

Competing interests

J.M., P.Y., R.L.M., and H.E.G. are named inventors on provisional patent entitled "Cell therapy for Alzheimer's disease" which is based on the Aβ-TCR sequence (EFS ID: 42475225, Application number: 63175747, Docket number: 21084P). H.E.G is a member of the scientific advisory board at Longevity Biotech and a co-founder of Exavir Therapeutics, Inc. All other authors declare no conflict of interest.

Author details

^{1}Department of Pharmacology and Experimental Neuroscience, University of Nebraska Medical Center, Omaha, Nebraska, USA.

References

1. Hansson O. Biomarkers for neurodegenerative diseases. Nat Med. 2021;27:954–63.
2. Villemagne VL, Burnham S, Bourgeat P, Brown B, Ellis KA, Salvado O, Szoeke C, Macaulay SL, Martins R, Maruff P, et al. Amyloid beta deposition, neurodegeneration, and cognitive decline in sporadic Alzheimer's disease: a prospective cohort study. Lancet Neurol. 2013;12:357–67.
3. Nordberg A. Mechanisms behind the neuroprotective actions of cholinesterase inhibitors in Alzheimer disease. Alzheimer Dis Assoc Disord. 2006;20:S12–8.
4. Cummings J, Lee G, Nahed P, Kambar M, Zhong K, Fonseca J, Taghva K. Alzheimer's disease drug development pipeline: 2022. Alzheimers Dement (N Y). 2022;8:e12295.

Yeapuri *et al. Molecular Neurodegeneration*   (2023) 18:97

Page 20 of 22

5. Schenk D, Barbour R, Dunn W, Gordon G, Grajeda H, Guido T, Hu K, Huang J, Johnson-Wood K, Khan K, et al. Immunization with amyloid-β attenuates Alzheimer-disease-like pathology in the PDAPP mouse. Nature. 1999;400:173–7.

6. Janus C, Pearson J, McLaurin J, Mathews PM, Jiang Y, Schmidt SD, Chishti MA, Horne P, Heslin D, French J, et al. Aβ peptide immunization reduces behavioural impairment and plaques in a model of Alzheimer's disease. Nature. 2000;408:979–82.

7. Morgan D, Diamond DM, Gottschall PE, Ugen KE, Dickey C, Hardy J, Duff K, Jantzen P, DiCarlo G, Wilcock D, et al. A beta peptide vaccination prevents memory loss in an animal model of Alzheimer's disease. Nature. 2000;408:982–5.

8. Orgogozo JM, Gilman S, Dartigues JF, Laurent B, Puel M, Kirby LC, Jouanny P, Dubois B, Eisner L, Flitman S, et al. Subacute meningoencephalitis in a subset of patients with AD after Abeta42 immunization. Neurology. 2003;61:46–54.

9. Nicoll JA, Wilkinson D, Holmes C, Steart P, Markham H, Weller RO. Neuropathology of human Alzheimer disease after immunization with amyloid-beta peptide: a case report. Nat Med. 2003;9:448–52.

10. Ferrer I, Boada Rovira M, Sánchez Guerra ML, Rey MJ, Costa-Jussá F. Neuropathology and pathogenesis of encephalitis following amyloid-beta immunization in Alzheimer's disease. Brain Pathol. 2004;14:11–20.

11. Monsonego A, Imitola J, Petrovic S, Zota V, Nemirovsky A, Baron R, Fisher Y, Owens T, Weiner HL. Abeta-induced meningoencephalitis is IFN-gamma-dependent and is associated with T cell-dependent clearance of Abeta in a mouse model of Alzheimer's disease. Proc Natl Acad Sci U S A. 2006;103:5048–53.

12. Ethell DW, Shippy D, Cao C, Cracchiolo JR, Runfeldt M, Blake B, Arendash GW. Aβ-specific T-cells reverse cognitive decline and synaptic loss in Alzheimer's mice. Neurobiol Dis. 2006;23:351–61.

13. Cao C, Arendash GW, Dickson A, Mamcarz MB, Lin X, Ethell DW. Aβ-specific Th2 cells provide cognitive and pathological benefits to Alzheimer's mice without infiltrating the CNS. Neurobiol Dis. 2009;34:63–70.

14. Jung M, Lee S, Park S, Hong J, Kim C, Cho I, Sohn HS, Kim K, Park IW, Yoon S, et al. A Therapeutic Nanovaccine that Generates Anti-Amyloid Antibodies and Amyloid-specific Regulatory T Cells for Alzheimer's Disease. Adv Mater. 2023;35:e2207719.

15. Pinti M, Appay V, Campisi J, Frasca D, Fulop T, Sauce D, Larbi A, Weinberger B, Cossarizza A. Aging of the immune system: Focus on inflammation and vaccination. Eur J Immunol. 2016;46:2286–301.

16. Salloway S, Chalkias S, Barkhof F, Burkett P, Barakos J, Purcell D, Suhy J, Forrestal F, Tian Y, Umans K, et al. Amyloid-related imaging abnormalities in 2 Phase 3 studies evaluating Aducanumab in patients with early Alzheimer Disease. JAMA Neurol. 2022;79:13–21.

17. van Dyck CH, Swanson CJ, Aisen P, Bateman RJ, Chen C, Gee M, Kanekiyo M, Li D, Reyderman L, Cohen S, et al. Lecanemab in early Alzheimer's disease. N Engl J Med. 2023;388:9–21.

18. Sperling RA, Jack CR Jr, Black SE, Frosch MP, Greenberg SM, Hyman BT, Scheltens P, Carrillo MC, Thies W, Bednar MM, et al. Amyloid-related imaging abnormalities in amyloid-modifying therapeutic trials: recommendations from the Alzheimer's Association Research Roundtable Workgroup. Alzheimers Dement. 2011;7:367–85.

19. Francesca A, Pawel K, Scott A: Accelerated brain volume loss caused by anti–β-amyloid drugs: a systematic review and meta-analysis. Neurology 2023:https://doi.org/10.1212/WNL.0000000000207156.

20. Shafer P, Kelly LM, Hoyos V. Cancer therapy with TCR-engineered T Cells: current strategies, challenges, and prospects. Front Immunol. 2022;13:835762.

21. Sterner RC, Sterner RM. CAR-T cell therapy: current limitations and potential strategies. Blood Cancer J. 2021;11:69.

22. Gate D, Saligrama N, Leventhal O, Yang AC, Unger MS, Middeldorp J, Chen K, Lehallier B, Channappa D, De Los Santos MB, et al. Clonally expanded CD8 T cells patrol the cerebrospinal fluid in Alzheimer's disease. Nature. 2020;577:399–404.

23. Oberstein TJ, Taha L, Spitzer P, Hellstern J, Herrmann M, Kornhuber J, Maler JM. Imbalance of circulating T(h)17 and regulatory T Cells in Alzheimer's disease: a case control study. Front Immunol. 2018;9:1213.

24. Larbi A, Pawelec G, Witkowski JM, Schipper HM, Derhovanessian E, Goldeck D, Fulop T. Dramatic shifts in circulating CD4 but not CD8 T Cell subsets in mild Alzheimer's disease. J Alzheimers Dis. 2009;17:91–103.

25. Anderson KM, Olson KE, Estes KA, Flanagan K, Gendelman HE, Mosley RL. Dual destructive and protective roles of adaptive immunity in neurodegenerative disorders. Translational Neurodegeneration. 2014;3:25.

26. Saresella M, Calabrese E, Marventano I, Piancone F, Gatti A, Alberoni M, Nemni R, Clerici M. Increased activity of Th-17 and Th-9 lymphocytes and a skewing of the post-thymic differentiation pathway are seen in Alzheimer's disease. Brain Behav Immun. 2011;25:539–47.

27. Cunningham C, Hennessy E. Co-morbidity and systemic inflammation as drivers of cognitive decline: new experimental models adopting a broader paradigm in dementia research. Alzheimers Res Ther. 2015;7:33.

28. Machhi J, Kevadiya BD, Muhammad IK, Herskovitz J, Olson KE, Mosley RL, Gendelman HE. Harnessing regulatory T cell neuroprotective activities for treatment of neurodegenerative disorders. Mol Neurodegener. 2020;15:32.

29. Faridar A, Thome AD, Zhao W, Thonhoff JR, Beers DR, Pascual B, Masdeu JC, Appel SH. Restoring regulatory T-cell dysfunction in Alzheimer's disease through ex vivo expansion. Brain Commun. 2020;2:fcaa112.

30. Faridar A, Vasquez M, Thome AD, Yin Z, Xuan H, Wang JH, Wen S, Li X, Thonhoff JR, Zhao W, et al. Ex vivo expanded human regulatory T cells modify neuroinflammation in a preclinical model of Alzheimer's disease. Acta Neuropathol Commun. 2022;10:144.

31. Yang H, Park SY, Baek H, Lee C, Chung G, Liu X, Lee JH, Kim B, Kwon M, Choi H, et al. Adoptive therapy with amyloid-beta specific regulatory T cells alleviates Alzheimer's disease. Theranostics. 2022;12:7668–80.

32. Olson KE, Namminga KL, Lu Y, Thurston MJ, Schwab AD, de Picciotto S, Tse SW, Walker W, Iacovelli J, Small C, et al. Granulocyte-macrophage colony-stimulating factor mRNA and Neuroprotective Immunity in Parkinson's disease. Biomaterials. 2021;272:120786.

33. Sakaguchi S, Yamaguchi T, Nomura T, Ono M. Regulatory T cells and immune toleranc. Cell. 2008;133:775–87.

34. Reynolds AD, Stone DK, Hutter JA, Benner EJ, Mosley RL, Gendelman HE. Regulatory T cells attenuate Th17 cell-mediated nigrostriatal dopaminergic neurodegeneration in a model of Parkinson's disease. J Immunol. 2010;184:2261–71.

35. Kiyota T, Machhi J, Lu Y, Dyavarshetty B, Nemati M, Yokoyama I, Mosley RL, Gendelman HE. Granulocyte-macrophage colony-stimulating factor neuroprotective activities in Alzheimer's disease mice. J Neuroimmunol. 2018;319:80–92.

36. Dansokho C, Ait Ahmed D, Aid S, Toly-Ndour C, Chaigneau T, Calle V, Cagnard N, Holzenberger M, Piaggio E, Aucouturier P, Dorothee G. Regulatory T cells delay disease progression in Alzheimer-like pathology. Brain. 2016;139:1237–51.

37. Olson KE, Namminga KL, Lu Y, Schwab AD, Thurston MJ, Abdelmoaty MM, Kumar V, Wojtkiewicz M, Obaro H, Santamaria P, et al. Safety, tolerability, and immune-biomarker profiling for year-long sargramostim treatment of Parkinson's disease. EBioMedicine. 2021;67:103380.

38. Gendelman HE, Zhang Y, Santamaria P, Olson KE, Schutt CR, Bhatti D, Shetty BLD, Lu Y, Estes KA, Standaert DG, et al. Evaluation of the safety and immunomodulatory effects of sargramostim in a randomized, double-blind phase 1 clinical Parkinson's disease trial. NPJ Parkinsons Dis. 2017;3:10.

39. Browne TC, McQuillan K, McManus RM, O'Reilly JA, Mills KH, Lynch MA. IFN-gamma Production by amyloid beta-specific Th1 cells promotes microglial activation and increases plaque burden in a mouse model of Alzheimer's disease. J Immunol. 2013;190:2241–51.

40. Olson KE, Abdelmoaty MM, Namminga KL, Lu Y, Obaro H, Santamaria P, Mosley RL, Gendelman HE. An open-label multiyear study of sargramostim-treated Parkinson's disease patients examining drug safety, tolerability, and immune biomarkers from limited case numbers. Transl Neurodegener. 2023;12:26.

41. Machhi J, Yeapuri P, Lu Y, Foster E, Chikhale R, Herskovitz J, Namminga KL, Olson KE, Abdelmoaty MM, Gao J, et al. CD4+ effector T cells accelerate Alzheimer's disease in mice. J Neuroinflammation. 2021;18:272.

42. Herskovitz J, Hasan M, Patel M, Blomberg WR, Cohen JD, Machhi J, Shahjin F, Mosley RL, McMillan J, Kevadiya BD, Gendelman HE. CRISPR-cas9 mediated exonic disruption for HIV-1 elimination. EBioMedicine. 2021;73:103678.

43. Hsiao K, Chapman P, Nilsen S, Eckman C, Harigaya Y, Younkin S, Yang F, Cole G. Correlative memory deficits, Abeta elevation, and amyloid plaques in transgenic mice. Science. 1996;274:99–103.

44. Duff K, Eckman C, Zehr C, Yu X, Prada C-M, Perez-tur J, Hutton M, Buee L, Harigaya Y, Yager D, et al. Increased amyloid-β42(43) in brains of mice expressing mutant presenilin 1. Nature. 1996;383:710–3.

45. Kiyota T, Machhi J, Lu Y, Dyavarshetty B, Nemati M, Zhang G, Mosley RL, Gelbard HA, Gendelman HE. URMC-099 facilitates amyloid-beta clearance in a murine model of Alzheimer's disease. J Neuroinflammation. 2018;15:137.

46. Kiyota T, Ingraham KL, Jacobsen MT, Xiong H, Ikezu T. FGF2 gene transfer restores hippocampal functions in mouse models of Alzheimer's disease and has therapeutic implications for neurocognitive disorders. Proc Natl Acad Sci U S A. 2011;108:E1339-1348.

47. Kiyota T, Okuyama S, Swan RJ, Jacobsen MT, Gendelman HE, Ikezu T. CNS expression of anti-inflammatory cytokine interleukin-4 attenuates Alzheimer's disease-like pathogenesis in APP+PS1 bigenic mice. FASEB J. 2010;24:3093–102.

48. Kiyota T, Gendelman HE, Weir RA, Higgins EE, Zhang G, Jain M. CCL2 affects beta-amyloidosis and progressive neurocognitive dysfunction in a mouse model of Alzheimer's disease. Neurobiol Aging. 2013;34:1060–8.

49. Prieur EAK, Jadavji NM. Assessing spatial working memory using the spontaneous alternation Y-maze test in aged male mice. Bio Protoc. 2019;9:e3162.

50. Yeapuri P, Olson KE, Lu Y, Abdelmoaty MM, Namminga KL, Markovic M, Machhi J, Mosley RL, Gendelman HE. Development of an extended half-life GM-CSF fusion protein for Parkinson's disease. J Control Release. 2022;348:951–65.

51. Livak KJ, Schmittgen TD. Analysis of relative gene expression data using real-time quantitative PCR and the 2(-Delta Delta C(T)) Method. Methods. 2001;25:402–8.

52. Niccoli T, Cabecinha M, Tillmann A, Kerr F, Wong CT, Cardenes D, Vincent AJ, Bettedi L, Li L, Gronke S, et al. Increased glucose transport into neurons rescues Abeta toxicity in Drosophila. Curr Biol. 2016;26:2291–300.

53. Hammond TC, Lin AL. Glucose metabolism is a better marker for predicting clinical Alzheimer's disease than amyloid or Tau. J Cell Immunol. 2022;4:15–8.

54. Ciccocioppo F, Lanuti P, Pierdomenico L, Simeone P, Bologna G, Ercolino E, Buttari F, Fantozzi R, Thomas A, Onofrj M, et al. The characterization of regulatory T-Cell profiles in Alzheimer's disease and Multiple sclerosis. Sci Rep. 2019;9:8788.

55. Abdelmoaty MM, Yeapuri P, Machhi J, Lu Y, Namminga KL, Kadry R, Lu E, Bhattarai S, Mosley RL, Gendelman HE. Immune senescence in aged APP/PS1 mice. NeuroImmune Pharm Ther. 2023;2:317–30.

56. Thonhoff JR, Beers DR, Zhao W, Pleitez M, Simpson EP, Berry JD, Cudkowicz ME, Appel SH. Expanded autologous regulatory T-lymphocyte infusions in ALS: A phase I, first-in-human study. Neurol Neuroimmunol Neuroinflamm. 2018;5:e465.

57. Hansen DV, Hanson JE, Sheng M. Microglia in Alzheimer's disease. J Cell Biol. 2018;217:459–72.

58. Butovsky O, Weiner HL. Microglial signatures and their role in health and disease. Nat Rev Neurosci. 2018;19:622–35.

59. Kamphuis W, Mamber C, Moeton M, Kooijman L, Sluijs JA, Jansen AH, Verveer M, de Groot LR, Smith VD, Rangarajan S, et al. GFAP isoforms in adult mouse brain with a focus on neurogenic astrocytes and reactive astrogliosis in mouse models of Alzheimer disease. PLoS ONE. 2012;7:e42823.

60. Monterey MD, Wei H, Wu X, Wu JQ. The Many Faces of Astrocytes in Alzheimer's Disease. Front Neurol. 2021;12:619626.

61. Lacorte E, Ancidoni A, Zaccaria V, Remoli G, Tariciotti L, Bellomo G, Sciancalepore F, Corbo M, Lombardo FL, Bacigalupo I, et al. Safety and efficacy of monoclonal antibodies for Alzheimer's disease: a systematic review and meta-analysis of published and unpublished clinical trials. J Alzheimers Dis. 2022;87:101–29.

62. Hu D, Xia W, Weiner HL. CD8(+) T cells in neurodegeneration: friend or foe? Mol Neurodegener. 2022;17:59.

63. Machado-Santos J, Saji E, Troscher AR, Paunovic M, Liblau R, Gabriely G, Bien CG, Bauer J, Lassmann H. The compartmentalized inflammatory response in the multiple sclerosis brain is composed of tissue-resident CD8+ T lymphocytes and B cells. Brain. 2018;141:2066–82.

64. Smolders J, Heutinck KM, Fransen NL, Remmerswaal EBM, Hombrink P, Ten Berge IJM, van Lier RAW, Huitinga I, Hamann J. Tissue-resident memory T cells populate the human brain. Nat Commun. 2018;9:4593.

65. Liston A, Dooley J, Yshii L. Brain-resident regulatory T cells and their role in health and disease. Immunol Lett. 2022;248:26–30.

66. Chwojnicki K, Iwaszkiewicz-Grześ D, Jankowska A, Zieliński M, Łowiec P, Gliwiński M, Grzywińska M, Kowalczyk K, Konarzewska A, Glasner P, et al. Administration of CD4+CD25highCD127−FoxP3+ regulatory T cells for relapsing-remitting Multiple sclerosis: a phase 1 study. BioDrugs. 2021;35:47–60.

67. Raffin C, Vo LT, Bluestone JA. T(reg) cell-based therapies: challenges and perspectives. Nat Rev Immunol. 2020;20:158–72.

68. Thornton AM, Shevach EM. Suppressor effector function of CD4+CD25+ immunoregulatory T cells is antigen nonspecific. J Immunol. 2000;164:183–90.

69. Tang Q, Henriksen KJ, Bi M, Finger EB, Szot G, Ye J, Masteller EL, McDevitt H, Bonyhadi M, Bluestone JA. In vitro–expanded antigen-specific regulatory T cells suppress autoimmune diabetes. J Exp Med. 2004;199:1455–65.

70. Tarbell KV, Yamazaki S, Olson K, Toy P, Steinman RM. CD25+ CD4+ T Cells, expanded with dendritic cells presenting a single autoantigenic peptide, suppress autoimmune diabetes. J Exp Med. 2004;199:1467–77.

71. Stephens LA, Malpass KH, Anderton SM. Curing CNS autoimmune disease with myelin-reactive Foxp3+ Treg. Eur J Immunol. 2009;39:1108–17.

72. Boardman DA, Philippeos C, Fruhwirth GO, Ibrahim MA, Hannen RF, Cooper D, Marelli-Berg FM, Watt FM, Lechler RI, Maher J, et al. Expression of a chimeric antigen receptor specific for donor HLA class I enhances the potency of human regulatory T cells in preventing human skin transplant rejection. Am J Transplant. 2017;17:931–43.

73. Bezie S, Charreau B, Vimond N, Lasselin J, Gerard N, Nerriere-Daguin V, Bellier-Waast F, Duteille F, Anegon I, Guillonneau C. Human CD8+ Tregs expressing a MHC-specific CAR display enhanced suppression of human skin rejection and GVHD in NSG mice. Blood Adv. 2019;3:3522–38.

74. Sagoo P, Ali N, Garg G, Nestle FO, Lechler RI, Lombardi G. Human regulatory T cells with alloantigen specificity are more potent inhibitors of alloimmune skin graft damage than polyclonal regulatory T cells. Sci Transl Med. 2011;3:83ra42.

75. Veerapathran A, Pidala J, Beato F, Yu X-Z, Anasetti C. Ex vivo expansion of human Tregs specific for alloantigens presented directly or indirectly. Blood. 2011;118:5671–80.

76. Brusko TM, Koya RC, Zhu S, Lee MR, Putnam AL, McClymont SA, Nishimura MI, Han S, Chang LJ, Atkinson MA, et al. Human antigen-specific regulatory T cells generated by T cell receptor gene transfer. PLoS ONE. 2010;5:e11726.

77. Hull CM, Nickolay LE, Estorninho M, Richardson MW, Riley JL, Peakman M, Maher J, Tree TI. Generation of human islet-specific regulatory T cells by TCR gene transfer. J Autoimmun. 2017;79:63–73.

78. Kerkar SP, Sanchez-Perez L, Yang S, Borman ZA, Muranski P, Ji Y, Chinnasamy D, Kaiser AD, Hinrichs CS, Klebanoff CA, et al. Genetic engineering of murine CD8+ and CD4+ T cells for preclinical adoptive immunotherapy studies. J Immunother. 2011;34:343–52.

79. Gershon RK, Kondo K. Infectious immunological tolerance. Immunology. 1971;21:903–14.

80. Gravano DM, Vignali DA. The battle against immunopathology: infectious tolerance mediated by regulatory T cells. Cell Mol Life Sci. 2012;69:1997–2008.

81. Legoux FP, Lim JB, Cauley AW, Dikiy S, Ertelt J, Mariani TJ, Sparwasser T, Way SS, Moon JJ. CD4+ T cell tolerance to tissue-restricted self antigens is mediated by antigen-specific regulatory T cells rather than deletion. Immunity. 2015;43:896–908.

82. Rutella S, Zavala F, Danese S, Kared H, Leone G. Granulocyte colony-stimulating factor: a novel mediator of T Cell tolerance. J Immunol. 2005;175:7085–91.

83. Silva-Filho JL, Caruso-Neves C, Pinheiro AAS. IL-4: an important cytokine in determining the fate of T cells. Biophys Rev. 2014;6:111–8.

84. Reale M, Iarlori C, Feliciani C, Gambi D. Peripheral chemokine receptors, their ligands, cytokines and Alzheimer's disease. J Alzheimers Dis. 2008;14:147–59.

85. Haar HJvd, Burgmans S, Jansen JFA, Osch MJPv, Buchem MAv, Muller M, Hofman PAM, Verhey FRJ, Backes WH. Blood-brain barrier leakage in patients with early Alzheimer disease. Radiology. 2016;281:527–35.

86. Chetelat G, Arbizu J, Barthel H, Garibotto V, Law I, Morbelli S, van de Giessen E, Agosta F, Barkhof F, Brooks DJ, et al. Amyloid-PET and (18)

Yeapuri *et al. Molecular Neurodegeneration*   (2023) 18:97

Page 22 of 22

F-FDG-PET in the diagnostic investigation of Alzheimer's disease and other dementias. Lancet Neurol. 2020;19:951–62.

87. Gordon BA, Blazey TM, Su Y, Hari-Raj A, Dincer A, Flores S, Christensen J, McDade E, Wang G, Xiong C, et al. Spatial patterns of neuroimaging biomarker change in individuals from families with autosomal dominant Alzheimer's disease: a longitudinal study. Lancet Neurol. 2018;17:241–50.

88. Nordberg A, Rinne JO, Kadir A, Langstrom B. The use of PET in Alzheimer disease. Nat Rev Neurol. 2010;6:78–87.

89. Mittal K, Eremenko E, Berner O, Elyahu Y, Strominger I, Apelblat D, Nemirovsky A, Spiegel I, Monsonego A. CD4 T cells induce a subset of MHCII-expressing microglia that attenuates Alzheimer pathology. iScience. 2019;16:298–311.

90. Xie L, Choudhury GR, Winters A, Yang SH, Jin K. Cerebral regulatory T cells restrain microglia/macrophage-mediated inflammatory responses via IL-10. Eur J Immunol. 2015;45:180–91.

Publisher's Note